hnRNPK-regulated *LINC00263* promotes malignant phenotypes through miR-147a/CAPN2

Woo Joo Lee
Sungkyunkwan University
Chang Hoon Shin
Sungkyunkwan University
Haein Ji
Sungkyunkwan University
Seong Dong Jeong
Sungkyunkwan University
Mi-So Park
Sungkyunkwan University
Hong-Hee Won
Sungkyunkwan University
Poonam Pandey
National Institute on Aging
Myriam Gorospe
National Institute on Aging
Hyeon Ho Kim (hyeonhkim@skku.edu)
Sungkyunkwan University https://orcid.org/0000-0002-0394-474X

Research

Keywords: Malignancy, hnRNPK, LINC00263, miR-147a, CAPN2

Posted Date: November 5th, 2020

DOI: https://doi.org/10.21203/rs.3.rs-100296/v1

Version of Record: A version of this preprint was published at Cell Death & Disease on March 17th, 2021.
See the published version at https://doi.org/10.1038/s41419-021-03575-1.

Abstract

Background: Malignant characteristics of cancers, represented by rapid cell proliferation and high metastatic potential, are a major cause of high cancer-related mortality. As a multifunctional RNA-binding protein, heterogeneous nuclear ribonucleoprotein K (hnRNPK) is closely associated with cancer progression in various types of cancers. In this study, we sought to identify hnRNPK-regulated long intergenic non-coding RNAs (lincRNAs) that play a critical role in the regulation of cancer malignancy.

Methods: Malignant phenotypes including metastatic and proliferative potential were examined using Transwell invasion assay, cell counting, and colony forming assay. To search for hnRNPK-regulated lincRNAs, RNA sequencing was performed. Using small RNA sequencing followed by antisense oligonucleotide pull-down, lincRNA-associated miRNAs were selected. The association between miRNA and target mRNA was determined by Argonaute 2-immunoprecipitation and luciferase reporter assay.

Results: We found that hnRNPK controlled malignant phenotypes including invasiveness, proliferation, and clonogenicity. RNA sequencing and functional studies revealed that *LINC00263*, a novel target of hnRNPK, is involved in the oncogenic functions of hnRNPK. Knockdown of *LINC00263* mitigated the malignant capabilities. Conversely, increased malignant phenotypes were observed in *LINC00263*-overexpressing cells. We also found that miR-147a negatively regulates *LINC00263* via direct interaction, thus suppressing malignant capabilities. Moreover, knockdown of hnRNPK and *LINC00263* upregulated miR-147a, indicating that *LINC00263* serves as a ceRNA for miR-147a. By analyzing RNA sequencing data and miRNA target prediction, calpain 2 (*CAPN2*) was identified as a putative target of miR-147a. Ago2-IP and luciferase reporter assay revealed that miR-147a suppressed CAPN2 expression by directly binding to the 3'UTR of *CAPN2* mRNA. Additionally, we found that the weakened malignant capabilities following knockdown of hnRNPK or *LINC00263* were restored by miR-147a inhibition or CAPN2 overexpression.

Conclusions: Our findings demonstrate that hnRNPK-regulated *LINC00263* plays an important role in cancer malignancy by acting as a miR-147a decoy and thus upregulating CAPN2.

Background

Malignant properties of cancer cells, including their highly aggressive characteristics, are major obstacles in the successful treatment of cancer. In fact, the degree of malignancy is a major factor that affects cancer mortality (1). Cell proliferation is an important part of cancer development and is tightly and precisely regulated by oncogenes and tumor suppressors. The limitless growth of cancer cells is a result of the abnormal activation of oncogenic signals that enhance the proliferation rate and inhibit apoptotic processes (2). Cancer metastasis involves multiple steps in which cancer cells are disseminated from primary site to other tissues or organs far from where they first occurred. Through the control of metastasis-associated genes, primary tumor cells prepare for metastasis by acquiring invasive capacity and proliferative properties to disseminate and survive in the secondary sites (3). Rapid proliferation and

metastatic potential are the main phenotypes associated with cancer malignancy. Therefore, the control of proliferation and metastasis is considered a promising approach for the development of cancer therapeutics.

Heterogeneous nuclear ribonucleoprotein K (hnRNPK) is a DNA- and RNA-binding protein that contains three K homology (KH) domains, a nuclear shuttling (KNS) domain, and a nuclear localization signal (NLS) (4). HnRNPK controls the expression of target genes mainly by directly binding to the untranslated region (UTR) of the target mRNAs. In addition, it is also known to influence gene expression through various other ways, such as transcription, splicing, and translation. Through a wide range of regulatory mechanisms, including post-transcriptional gene regulation, hnRNPK is known to induce genes involved in extracellular matrix, cell motility, and angiogenesis (5, 6). Furthermore, a loss-of-function screening using randomized intracellular antibodies has revealed that hnRNPK is a potential target for metastasis therapy and its cytoplasmic accumulation is crucial for its role in metastasis (7). We previously reported hat hnRNPK regulates proliferation of cancer cells by targeting polo-like kinase 1 (*PLK1*) and heme oxygenase-1 (*HO-1*). Further, we demonstrated that mechanically, hnRNPK competes for interaction with *PLK1* mRNA (8) and increases the expression of *HO-1* through *PTOV1*-miR-1207-5p (9).

MicroRNAs (miRNAs) typically regulate gene expression at the post-transcriptional level by recognizing miRNA-recognition elements (MREs) within their target mRNA. Non-coding RNAs (ncRNAs) may share MREs with target mRNA of coding genes and therefore be targeted by miRNAs. This interaction and sequestering of miRNA by ncRNAs constitutes the basis for the competitive endogenous RNA (ceRNA) theory (10). Recently, long non-coding RNAs (lncRNAs) have received increasing attention for their key roles in cancer progression as oncogenes and tumor suppressors (11). Moreover, accumulating evidence suggests that lncRNAs play a crucial role in cancer metastasis (12). In the nucleus, lncRNAs are involved in the formation of ribonucleoprotein complexes or recruitment of chromatin remodeling complexes by acting as scaffolds or guides. In addition to their roles in the nucleus, lncRNAs regulate target gene expression by functioning as ceRNAs that competitively bind to target mRNA with miRNAs. Therefore, lncRNAs mitigate miRNA-mediated repression of target genes. Emerging evidences suggest that ceRNA-mediated gene regulatory network is closely associated with cancer progression in various types of cancers.

In this study, we screened hnRNPK-regulated lncRNAs that are responsible for the oncogenic function of hnRNPK. *LINC00263* was identified as a novel target of hnRNPK and potentiates malignant properties including proliferation and invasiveness by functioning as a decoy for miR-147a and thus upregulating calpain 2 (*CAPN2*) expression.

Materials And Methods

Cell culture and transfection

Human cervical cancer (HeLa) cells were maintained in Dulbecco's modified Eagle's medium (Hyclone, Logan, UT, USA). Human non-small cell lung cancer (H460 and H1299), human colon cancer (DLD1 and

LoVo), human melanoma (A375P), and human neuroblastoma (T98G and A172) cells were maintained with RPMI 1640 medium (GIBCO-BRL, Grand Island, NY, USA). Both culture media were supplemented with 10% fetal bovine serum (GIBCO-BRL, Grand Island, NY) and 1% antibiotic-antimycotic solution (GIBCO-BRL). For siRNA transfection, cells were plated at 60% density and transfected with the indicated siRNAs using Lipofectamine2000 (Invitrogen, Thermo Fisher Scientific, Waltham, MA) according to the manufacturer's protocol. The siRNAs for *HNRNPK* and *LINC00263* were synthesized by Bioneer (Daejeon, Republic of Korea; sequences are shown in Supplementary table 1). *CAPN2*-targeting siRNA were purchased from Santa Cruz Biotechnology (sc-41459: Santa Cruz, CA). Precursor miR-147a (pre-miR-147a: PM10020) and antisense miR-147a (anti-miR-147a: AM10020) were purchased from Ambion (Ambion, Thermo Fisher Scientific, Waltham, MA) and used for overexpression or inhibition of miR-147a, respectively, using Lipofectamine2000 (Invitrogen).

Western blot analysis

Cells were lysed using radioimmunoprecipitation (RIPA) buffer containing protease and phosphatase inhibitors (Roche, Basel, Switzerland). Equal amounts of the cell lysate were separated by dodium dodecyl sulfate-polyacrylamide gel electrophoresis (SDS-PAGE) and transferred to polyvinylidene difluoride membranes (Millipore, Billerica, MA). After blocking with 5% skim milk, the membranes were incubated with the indicated primary antibody (Supplementary table 2), washed with tris-buffered saline containing tween-20, and incubated with the appropriate secondary antibody. The protein bands were detected using enhanced chemiluminescent reagent. GAPDH was used as a loading control.

Reverse transcription-quantitative polymerase chain reaction (RT-qPCR) analysis

Total RNA was isolated using TRIzol (Invitrogen) according to the manufacturer's instructions and used as a template to synthesize cDNA, using the SuperScript III First-Strand Synthesis System (Invitrogen). The expression levels of mRNAs were quantified by RT-qPCR analysis with appropriate primers (sequences are shown in Supplementary table 3) using the Power SYBR Green PCR Master Mix (Applied Biosystems, Foster City, CA). To determine the stability of *LINC00263*, cells were transfected with control and HNRNPK siRNA. Following treatment of actinomycin D (0.5 mg/ml), cells were harvested at the indicated times and the levels of *LINC00263* and *GAPDH* mRNA were determined by RT-qPCR analysis.

Determination of malignant phenotypes

The invasive ability of the cells was determined using the BD Biocoat™ Matrigel invasion chamber (BD Bioscience, San Jose, CA). Equal number of transfected cells in serum-free media were added into the upper chamber. Invasion was triggered by adding the same medium supplemented with 10% FBS to the bottom chambers as a chemoattractant. After incubation for 24 h, the invaded cells were fixed with 95% MeOH for 5 min and stained with 0.1% hematoxylin and eosin. Invasiveness was determined by counting the number of invaded cells in at least ten randomly selected fields. For analysis of cell proliferation rate, the transfected cells were plated in 6-well plates at a density of $5 \times 10^4 - 1 \times 10^5$ cells/well. Cells were trypsinized and the number of viable cells were assessed under a microscope at the indicated time

points. For clonogenicity assay, the transfected cells were plated in triplicate in 6-well plates and cultured for 2 weeks. Cells were fixed with 4% paraformaldehyde and stained with 0.2% crystal violet. The stained colonies were counted using Image J program.

Cellular fractionation

Cellular fractionation assay was performed to determine the subcellular localization of *LINC00263* (8). Briefly, HeLa cells were lysed with RSB buffer (10 mM Tris-HCl, pH 7.4, 2.5 mM $MgCl_2$, 100 mM NaCl) containing 4 mg/ml digitonin (BN2006, Thermo Fisher Scientific). After centrifugation, the supernatant was collected as the cytosolic extract. The remaining nuclear pellet was washed five times with RSB buffer and then lysed with RIPA buffer. The protein levels of α-tubulin and lamin B served as markers for the cytosolic and nuclear fraction, respectively.

Ribonucleoprotein immunoprecipitation

The association of hnRNPK with *LINC00263* was assessed by ribonucleoprotein immunoprecipitation (RNP-IP) using hnRNPK-specific antibody (ChIP grade) as described in our previous report (8). In case of direct interaction between miRNA and its targets, we used antibody recognizing Argonaute 2 (Ago2). Dynabeads™ Protein G (Invitrogen) was coupled with the indicated antibody followed by incubation of cytoplasmic lysate prepared using polysome extraction buffer with the antibody-conjugated beads. Following treatment with DNase I and protease K, RNAs were isolated from beads and the enrichment of target RNA level was determined by RT-qPCR analysis. The level of *18S* was used for normalization in all RNP-IP experiments. Details of the antibodies and primers used are provided Supplementary table 2-3.

Antisense oligonucleotide (ASO) pull-down assay

To identify LINC00263-associated miRNAs, ASO pull-down was performed using non-overlapping biotinylated ASOs recognizing *LacZ* (four ASOs) and *LINC00263* (eight ASOs). Incubation of the whole cell lysates with the biotinylated ASO was followed by coupling with Streptavidin-coupled Dynabeads™ (Invitrogen). RNAs were isolated from the pull-down materials and small RNA sequencing was performed.

Luciferase reporter assay

To verify the direct interaction between miR-147a and MRE in its target, pmirGLO dual-luciferase vectors (E133A, Promega, Madison, WI) containing wild-type or mutant MRE sequences from *LINC00263* or *CAPN2* mRNA were constructed. Following transfection with control or pre-miR-147a, equal number of HeLa cells were plated into 24-well plates. Then the cells were transfected with either wild-type or mutant luciferase vector. Luciferase expression was assessed using a Dual-GLO™ Luciferase Assay System (E2940, Promega).

Results

hnRNPK is responsible for the malignant phenotypes of cancer cells

We investigated the role of hnRNPK in malignant phenotypes including metastatic potential and proliferation in HeLa cells. To investigate the role of hnRNPK in cancer malignancy, two independent *HNRNPK*-specific siRNAs were designed and introduced into HeLa cells. For overexpression of hnRNPK, we used a pcDNA/Flag-hnRNPK vector constructed previously (8). Individual and mixture of *HNRNPK* siRNAs efficiently decreased hnRNPK expression (Fig. 1a). Conversely, introduction of Flag-hnRNPK resulted in a significant increase of hnRNPK in a dose-dependent manner (Fig. 1b). Using the siRNAs, we tested the effect of knockdown of hnRNPK on the invasiveness of HeLa cells. The invasive ability was reduced by approximately 65% (siRNA #1), 52% (siRNA #2), and 54% (mixed siRNA), respectively, compared to the control siRNA (Fig. 1c). Conversely, overexpression of hnRNPK enhanced the invasive ability by approximately 1.8–2.7-fold compared to the blank Flag vector (Fig. 1d), indicating that hnRNPK is closely associated with the invasiveness of cancer cells.

Two other distinctive features of malignancy, the proliferation rate and clonogenicity, were also examined. We observed that knockdown of hnRNPK using two individual siRNAs or a mixture resulted in a decrease in the proliferation rate (Fig. 1e). On the other hand, hnRNPK-overexpressing cells showed higher proliferation rate than the blank vector control cells (Fig. 1f). Next, we examined the colony forming ability following knockdown or overexpression of hnRNP. Knockdown of hnRNPK abrogated the colony forming ability to less than 50% of the control (Fig. 1g). In contrast, the number of colonies was dose-dependently increased following hnRNPK overexpression (Fig. 1h). These results showed that increased hnRNPK resulted in higher proliferative potential. Collectively, our findings demonstrate that hnRNPK is responsible for the malignant characteristics including high invasiveness and rapid proliferation.

LINC00263 is identified as a novel hnRNPK-regulated lincRNA

We hypothesized that long intergenic non-coding RNAs (lincRNAs) are involved in hnRNPK-mediated cancer malignancy. To identify hnRNPK-regulated lincRNAs, we performed RNA sequencing using hnRNPK-silenced HeLa cells. The various plots representing RNA sequencing data (scatter plot, volcano plot, and volume plot) and gene ontology (GO) analysis are shown in Supplementary Fig. 1a and 1c. Based on the data analysis and processing, five lincRNAs were identified to be significantly regulated by hnRNPK (Fig. 2a and 2b). Of the five lincRNAs, two lincRNAs, *LINC00618* and *LINC02246* were upregulated following knockdown of hnRNPK. In contrast, the expression levels of *LINC01137*, *LINC00263*, and *LINC00162* were lower in hnRNPK-silenced cells than in control cells. Since *LINC00263* showed the most significant effect on the metastatic potential (data not shown) of the cells, we chose to investigate its role in the control of cancer malignancy through hnRNPK.

To verify the RNA sequencing data, we performed transient knockdown of hnRNPK and observed substantial decrease in hnRNPK expression with two individual siRNAs (Fig. 2c). Further, knockdown of

hnRNPK also reduced the level of *LINC00263* significantly (Fig. 2d). We next sought to determine whether *LINC00263* affects hnRNPK expression. Following transient transfection of cells with two independent *LINC00263*-specific siRNAs, the levels of *HNRNPK* mRNA and *LINC00263* were determined by RT-qPCR analysis. Although both *LINC00263*-targeting siRNAs caused a substantial decrease in *LINC00263* level, they did not affect the levels of hnRNPK protein and mRNA (Fig. 2e and 2f, respectively). In addition, a specific siRNA targeting the 3'UTR of the *HNRNPK* mRNA was designed and introduced into HeLa cells with Flag-hnRNPK overexpression vector. Knockdown of hnRNPK by 3'UTR-targeting siRNA efficiently decreased the expression of hnRNPK without significant change in the ectopic hnRNPK (Flag-hnRNPK) (Fig. 2g). In accordance with previous results, introduction of the 3'UTR-targeting siRNA resulted in decreased expression of *LINC00263*. However, the level of *LINC00263* was restored to control level following ectopic expression of hnRNPK (Fig. 2h).

From above results, we identified LINC00263 as a novel hnRNPK-regulated lincRNA. Therefore, we investigated detailed molecular mechanism by which hnRNPK regulates the expression of *LINC00263*. Since five hnRNPK motives are predicted in the sequence of *LINC00263* using a bioinformatic tool for RBP binding site prediction (http://rbpmap.technion.ac.il/) (Supplementary Fig. 2a and 2b), the direct interaction between hnRNPK and *LINC00263* was examined through RNP-IP experiment. *LINC00263* was found to be highly enriched approximately 20-fold in endogenous hnRNPK IP material compare to control IgG (Fig. 2i). In addition, RNP-IP using full-length Flag-hnRNPK and its various deletion mutants (ΔKH1, ΔKH1/2, ΔKH2, and ΔKH3) revealed that interaction of hnRNPK with *LINC00263* was dependent on its K homology 1 (KH1) and KH2 domains (Fig. 2j). These results suggested that hnRNPK might regulate *LINC00263* at post-transcriptional level. Therefore, we examined whether hnRNPK influences the stability of *LINC00263* (Fig. 2k). Knockdown of hnRNPK induced more rapid decrease in *LINC00263* compare to control. The approximate half-life of *LINC00263* in control and hnRNPK-silenced cells was calculated as 13.5 h and 7.6 h, respectively. However, the level of *GAPDH* mRNA was barely affected by knockdown of hnRNPK. Collectively, we demonstrate that hnRNPK stabilized *LINC00263* through direct interaction and *LINC00263* is a novel target of hnRNPK.

LINC00263 promotes malignant phenotypes including invasiveness, proliferation, and clonogenicity

To investigate whether *LINC00263* is responsible for hnRNPK-mediated invasiveness, we performed transient knockdown or overexpression of *LINC00263* and examined the invasive ability of the cells using Transwell invasion assay. Knockdown of *LINC00263* in HeLa cells using two independent siRNAs resulted in approximately 50% decrease in the number of invading cells (Fig. 3a). Conversely, overexpression of *LINC00263* potentiated the invasive ability of HeLa cells in a dose-dependent manner (Fig. 3b). The level of *LINC00263* in the overexpressing cells was verified by RT-qPCR analysis (Supplementary Fig. 3a). Next, the proliferation rate and clonogenicity were assessed in *LINC00263*-silenced and -overexpressing HeLa cells. We observed decreased proliferation rate in *LINC00263*-silenced cells by two individual siRNAs (Fig. 3c). In contrast, the proliferation rate tended to increase in a dose-dependent manner in *LINC00263*-overexpressing cells (Fig. 3d). We also examined the effect of *LINC00263* knockdown on colony forming ability of the cells. We found that approximately 40% decrease

in the number of colonies in two individual siRNA-transfected cells (Fig. 3e), while the colony forming ability was increased following overexpression of *LINC00263* (Fig. 3f). These results indicate that *LINC00263* is associated with the oncogenic function of hnRNPK.

miR-147a is involved in the regulation of cancer malignancy by hnRNPK/ LINC00263

To determine the molecular mechanism through which *LINC00263* positively regulates malignant properties, we first examined the subcellular localization of *LINC00263* using cellular fractionation assay. For verification of the appropriate cellular fractions, the levels of a-tubulin (cytosolic marker) and lamin B (nuclear marker) were analyzed in each fraction by Western blot analysis (Fig. 4a). The level of *LINC00263* in each fraction was determined by RT-qPCR analysis. The levels of *18S*, *GAPDH*, and *ACTB* mRNA were assessed for reference (Fig. 4b). The cellular fractionation assay revealed that *LINC00263* was mainly localized in the cytosolic fraction. Additionally, we performed Argonaute 2 immunoprecipitation (Ago2-IP) assay to examine whether *LINC00263* was associated with the function of miRNAs (Fig. 4c). *LINC00263* was more enriched in Ago2-IP compared to control IgG-IP, indicating that *LINC00263* is involved in the regulatory pathway of miRNAs (results of three independent experiments are shown in Supplementary Fig. 5a).

From the above results, we concluded that *LINC00263* is mainly located in the cytosol and co-immunoprecipitated with Ago2 antibody, which suggests that *LINC00263* may function as a competitive endogenous RNA (ceRNA) for miRNA. Therefore, we hypothesized that *LINC00263* might be closely involved in the oncogenic function of hnRNPK by sponging tumor-suppressor miRNAs. To identify *LINC00263*-associated miRNAs, seven ASOs consisting of complementary sequences of *LINC00263* were designed to perform ASO pull-down experiments. Four ASOs for *LacZ* were used for control IP (Fig. 4d and Supplementary Fig. 4a). To test the efficiency of the ASO pull-down, the levels of *LINC00263* and *ACTB* mRNA in ASO pull-down materials were determined by RT-qPCR analysis. Whereas *ACTB* mRNA was not enriched, *LINC00263* was selectively enriched in the pull-down materials using the corresponding ASOs as compared to *LacZ* ASO (Fig. 4e). To screen *LINC00263*-bound miRNAs, small RNA sequencing was performed using the RNA isolated from the ASO pull-down. Analysis of sequencing data revealed that 24 miRNAs showed higher enrichment in *LINC00263* ASO pull-down material than in *LacZ* ASO pull-down, suggesting that they bound to *LINC00263* directly or indirectly (Fig. 4f and Supplementary Fig. 4b). Next we predicted the potential miRNA binding sites within *LINC00263* sequence using a miRNA target discovery tool RNA22 (https://cm.jefferson.edu/rna22). This bioinformatic tool revealed that *LINC00263* possessed MREs for only four miRNAs (miR-147a, miR-492, miR-601, and miR-1268a) out of the 24 miRNAs found by the ASO pull-down analyses (Supplementary Fig. 4c). Since miR-147a showed the most significant folding energy, we chose to further investigate whether miR-147a was responsible for the oncogenic function of hnRNPK/*LINC00263*.

To confirm the interaction between miR-147a and *LINC00263*, we examined the enrichment of *LINC00263* in Ago2-IP. Precursor miR-147a (pre-miR-147a) was used for overexpression and the level of miR-147a in transfected cells was found to be markedly increased (Supplementary Fig. 3b). Ago2-IP assay indicated

that overexpression of miR-147a resulted in an increase in *LINC00263* in Ago2 IP materials, indicating that miR-147a guided the interaction of *LINC00263* with Ago2 to form miRNA-induced silencing complex (miRISC) (Fig. 4g). In contrast, inhibition of miR-147a using anti-miR-147a (Supplementary Fig. 3c) decreased the level of *LINC00263* in Ago2-IP (Fig. 4h). These results indicate that *LINC00263* is associated with miR-147a-guided RISC. Therefore, we analyzed whether miR-147a regulated *LINC00263* expression. Decreased level of *LINC00263* was observed in miR-147a-overexpressing cells compared to that in the control (Fig. 4i); conversely, *LINC00263* was highly expressed following miR-147a knockdown using anti-miR-147a (Fig. 4j). In general, the reduction of a ceRNA leads to an increase in the ceRNA-bound miRNAs, thus the repressing function of miRNA is potentiated in ceRNA-silenced cells. Accordingly, we assessed the level of miR-147a in hnRNPK- and *LINC00263*-silenced cells (Fig. 4k). Knockdown of both hnRNPK and *LINC00263* resulted in approximately 2-fold increase of miR-147a, indicating that *LINC00263* acts as a ceRNA for miR-147a. Two MREs of miR-147a in *LINC00263* were predicted by bioinformatic tool (Supplementary Fig. 7a and 7b). Consequently, we constructed luciferase reporter vectors containing wild-type or mutant sequence of miR-147a MREs. In both reporter vectors, overexpression of miR-147a suppressed the expression of luciferase in wild-type reporter vector but not in the mutant (Fig. 4l). The results of Ago2-IP and luciferase reporter assay suggest that miR-147a directly binds to *LINC00263*.

Next, we tested whether miR-147a influences malignant phenotypes. Invasiveness was reduced to less than 30% of the control following overexpression of miR-147a; conversely, inhibition of miR-147a using anti-miR-147a resulted in approximately 4-fold increased invasive ability (Fig. 4m and 4n, respectively). In addition to invasiveness, proliferation rate and colony forming ability were also regulated by miR-147a. Under conditions of high miR-147a levels, the proliferation rate and clonogenicity were diminished (Fig. 4o and 4q, respectively). On the other hand, decrease in miR-147a level resulted in higher proliferative and clonogenic abilities compared to those of the control (Fig. 4p and 4r, respectively). Collectively, we concluded that *LINC00263* controls malignant properties by functioning as a ceRNA of the tumor-suppressor, miR-147a.

CAPN2 is a target of hnRNPK/ LINC00263 /miR-147a axis

To search for target genes responsible for the oncogenic function of hnRNPK/*LINC00263*/miR-147a, we conducted RNA sequencing using total RNA isolated from hnRNPK- and *LINC00263*-silenced HeLa cells (Supplementary Fig. 1a and 1b) and tried to identify common target genes. TargetScan (http://www.targetscan.org) was used to predict miR-147a target genes. As shown in Fig. 5a, eight genes (*CAPN2*, *CCND1*, *CDKN1A*, *CSDC2*, *L1CAM*, *PAQR4*, *PARP12*, and *TRIM47*) were identified as common target genes that are simultaneously regulated by hnRNPK, *LINC00263*, and miR-147a. RT-qPCR analysis indicated that knockdown of either hnRNPK or *LINC00263* significantly decreased the level of *CAPN2* mRNA, suggesting that it may be a putative target of hnRNPK/*LINC00263*/miR-147a (Supplementary Fig. 6). To check the possibility that hnRNPK regulates CAPN2 by directly binding to *CAPN2* mRNA, RNP-IP experiment was performed. Whereas *LINC00263* was highly enriched in hnRNPK IP material, *CAPN2* mRNA was barely bound to hnRNPK (Fig. 5b), indicating that hnRNPK regulates the expression of CAPN2

in an indirect way. Subsequently, we examined the role of hnRNPK/*LINC00263*/miR-147a in regulating CAPN2 expression. Overexpression of miR-147a resulted in decreased *CAPN2* protein expression without any change in hnRNPK. Consistent with the results of the Western blot and RT-qPCR analyses, overexpression of miR-147a decreased the level of *CAPN2* mRNA (Fig. 5c). Conversely, inhibition of miR-147a using anti-miR-147a resulted in increased CAPN2 protein and mRNA expression (Fig. 5d). Overexpression and inhibition efficiencies of the pre-miR-147a and anti-miR-147a, respectively, were confirmed by determining the level of miR-147a by RT-qPCR analysis (Supplementary Fig. 3b and 3c, respectively). To determine direct binding between *CAPN2* mRNA and miR-147a, the level of *CAPN2* mRNA in Ago2-IP material was assessed. Ago2-IP revealed that miR-147a increased the enrichment of *CAPN2* mRNA in miRISC (Fig. 5e); conversely, knockdown of miR-147a using antisense miRNA decreased the level of CAPN2 mRNA in the Ago2-IP material (Fig. 5f). In addition to Ago2-IP, luciferase reporter vectors containing the wild-type and mutant MRE of miR-147a were constructed to confirm the direct binding of miR-147a to the 3'UTR of *CAPN2* mRNA. Overexpression of miR-147a inhibited luciferase activity in wild-type vector, whereas it did not affect the expression of luciferase in mutant vector (Fig. 5g).

Next, we tested the effect of hnRNPK and *LINC00263* silencing on CAPN2 expression. Knockdown of hnRNPK and *LINC00263* significantly decreased the level of CAPN2 protein and mRNA (Fig. 5h). *CAPN2* mRNA was enriched in Ago2-IP following knockdown of hnRNPK or *LINC00263* (Fig. 5i). These results indicated that decrease in hnRNPK strengthens the function of miR-147a by reducing *LINC00263*, a ceRNA of miR-147a. To validate whether CAPN2 is involved in the regulation of malignant phenotypes by hnRNPK/*LINC00263*/miR-147a, the effect of CAPN2 silencing on invasiveness, proliferation, and clonogenicity was examined. Introduction of *CAPN2*-specific siRNA into HeLa cells markedly decreased CAPN2 expression (Fig. 5j). As expected, knockdown of CAPN2 decreased the number of invading cells (Fig. 5k), inhibited cell proliferation (Fig. 5l), and suppressed colony forming ability (Fig. 5m). Collectively, we demonstrated that CAPN2 was responsible for the oncogenic function as a target of hnRNPK/*LINC00263*/miR-147a.

Extracellular signal-regulated kinase (ERK) and p70S6K pathways are involved in the function of hnRNPK/ LINC00263 /miR-147a/CAPN2

The proteome profiler human p-kinase array was used to identify common signaling pathways of the hnRNPK/*LINC00263*/miR-147a/CAPN2 axis. Phosphorylation of ERK and p70S6K was found to be diminished in *HNRNPK*- or *LINC00263*-silenced cells compared to the controls (Supplementary Fig. 8a and 8b). To verify this observation, the levels of p-ERK and p-p70S6K were assessed. Western blot analysis indicated that knockdown of hnRNPK or *LINC00263* reduced phosphorylated ERK and p70S6K. Further, decreased expression of *CAPN2* using miR-147a or siRNA inhibit the activation of ERK and p70S6K (Supplementary Fig. 8c). These results demonstrate that ERK and p70S6K pathways are closely involved in the function of hnRNPK/*LINC00263*/miR-147a/CAPN2.

Repression of malignant capabilities is restored by miR-147a inhibition or CAPN2 overexpression

From the above results, we found that hnRNPK-regulated *LINC00263* decoys miR-147a and thus increases CAPN2 expression. To verify our findings, we performed rescue experiments by downregulating miR147-a using anti-miR-147a. HeLa cells were transfected with *HNRNPK* or *LINC00263* siRNA and with anti-miR-147a. RT-qPCR analysis results showed the level of miR-147a was efficiently decreased following introduction of anti-miR-147a. The level of miR-147a was significantly decreased not only in the control but also in hnRNPK- or *LINC00263*-silenced cells where miR-147a is upregulated by lowering its ceRNA, *LINC00263* (Fig. 6a). Whereas knockdown of hnRNPK or *LINC00263* increased the level of *CAPN2* mRNA in Ago2 IP, the inhibition of miR-147a by anti-miRNA lowered the enrichment of *CAPN2* mRNA in miRISC, indicating that miR-147a is responsible for the repression of CAPN2 in hnRNPK- and *LINC00263*-silenced cells (Fig. 6b). Subsequently, we analyzed the level of CAPN2 protein and mRNA in transfected cells. Inhibition of miR-147a using anti-miRNA reversed the decrease in CAPN2 protein and mRNA caused by the knockdown of hnRNPK and *LINC00263* as well (Fig. 6c). Next, we tested the effect of anti-miR-147a on invasiveness and clonogenicity. Consistent with the recovery of reduced CAPN2 expression, invasiveness and colony forming abilities were restored by anti-miR-147a (Fig. 6d and 6e, respectively). These results demonstrate that miR-147a is closely involved in the regulation of CAPN2 expression, and thus plays an important role in the gain of malignant phenotypes by hnRNPK/*LINC00263*.

In addition to inhibition of miR-147a, we examined whether the ectopic expression of CAPN2 reverses the lowered malignant capabilities resulting from the knockdown of hnRNPK and *LINC00263*. The appropriate concentration of overexpression vector was determined by introducing various concentrations of Flag-CAPN2 vector (Supplementary Fig. 3d). For the rescue experiment, HeLa cells were simultaneously transfected with Flag-CAPN2 vector and *HNRNPK*- or *LINC00263*-targeting siRNA. Western blot analysis showed that knockdown of hnRNPK and *LINC00263* decreased CAPN2 expression and that ectopic CAPN2 did not affect the expression of hnRNPK (Fig. 6f). Invasive and clonogenic abilities were also examined under the same conditions. As observed earlier, invasiveness was significantly decreased following the knockdown of hnRNPK and *LINC00263*. However, following ectopic overexpression of CAPN2, the invasive ability was restored (Fig. 6g). Consistent with the results of invasion assay, the colony forming assay revealed that ectopic CAPN2 restored the clonogenic ability that was reduced in the hnRNPK- and *LINC00263*-silenced cells (Fig. 6h). Collectively, we concluded that CAPN2 is a major effector of the oncogenic function of hnRNPK/*LINC00263*/miR-147a.

hnRNPK/ LINC00263 **/miR-147a/CAPN2 axis is applicable to various types of cancer cells**

To generalize our findings to various types of cancer cells, the regulatory action of hnRNPK/*LINC00263*/miR-147a/CAPN2 was examined in two lung cancer cells (H460 and H1299). *LINC00263* was recently reported to be abnormally regulated and play an important role in the progression of lung cancer cells (13). Therefore, we compared the level of *LINC00263* in two GSE datasets (Supplementary Fig. 9a and 9b). *LINC00263* was highly expressed in non-small cell lung cancer tissues compared to non-malignant tissues (GSE81089) and in tumor tissues compared to normal (GSE40419) tissues. To confirm the observations of the GSE dataset, we compared the level of *HNRNPK* mRNA and *LINC00263* in two lung cancer cells (H460 and H1299) with those in non-cancerous WI-38

cells (Fig. 7a). Compared to that in WI-38 cells, the expression of *HNRNPK* and *LINC00263* was significantly increased in both the lung cancer cells. Further, the expression level of *HNRNPK* mRNA and *LINC00263* was positively correlated. Interestingly, H1299 cells showed higher invasive ability than H460 cells (Supplementary Fig. 9c), indicating that the higher the invasiveness, the greater the increase of *HNRNPK* mRNA and *LINC00263*. Consistent with the previous results, knockdown of hnRNPK and *LINC00263* induced a decrease of CAPN2 mRNA in both the lung cancer cells (Fig. 7c). In addition to *HNRNPK* and *LINC00263* siRNA, introduction of pre-miR-147a and *CAPN2* siRNA into H460 and H1299 cells also decreased the expression of CAPN2 (Fig. 7d). As expected, the invasive and clonogenic abilities were diminished following knockdown of hnRNPK and *LINC00263* (Fig. 7e). Since H460 cells exhibited relatively lower expression of LINC00263, we tested whether overexpression of *LINC00263* potentiates invasive ability (Supplementary Fig. 9d). We found that *LINC00263* increased the number of invading cells in a dose-dependent manner. The number of colonies was also decreased in *HNRNPK*- and *LINC00263*-silenced cells (Fig. 7f). Overexpression of miR-147a by introducing pre-miR-147a lowered invasive and colony forming abilities of both the lung cancer cells (Fig. 7g and 7 h, respectively). Conversely, inhibition of miR-147a using anti-miR-147a induced an increase in the invasiveness and clonogenicity. The oncogenic function of CAPN2 was verified by assessing the number of invading cells and colonies in CAPN2-silenced cells. From these results, we confirmed that hnRNPK/*LINC00263*/miR-147a/CAPN2 regulatory axis is very closely related to the malignant phenotype of lung cancer cells.

Next, the role of hnRNPK/*LINC00263*/miR-147a in regulation of CAPN2 expression was verified in various other cancer cells including DLD1 and LoVo (colon cancer), A375 (melanoma), T98G (neuroblastoma), and A172 (astrocytoma) cells. All the cells tested showed suppression of CAPN2 expression as observed in HeLa and lung cancer cells. Briefly, CAPN2 expression was decreased in hnRNPK- or *LINC00263*-silenced cells. In addition, overexpression of miR-147a also resulted in suppression of CAPN2. From above results, we confirmed that our findings are applicable to various types of cancers.

Discussion

Cancer malignancy, the main cause of high cancer-related mortality, is controlled by strict and precise control of gene expression. Accumulating evidences indicates that RNA-binding proteins (RBPs) and non-coding RNAs (ncRNAs) are key players in post-transcriptional gene regulation by affecting multiple steps of gene expression such as splicing, mRNA export, mRNA localization, mRNA stability, and translation (14). RBPs and ncRNAs are also known to modulate multiple cancer traits related to cancer progression, for instance, rapid proliferation and high metastatic potential. hnRNPK is known to be one of the most promising RBP targets for the treatment of various cancers. Typically, hnRNPK accelerates cellular proliferation and potentiates metastatic potential by upregulating a wide range of oncogenes that trigger malignant phenotypes. Recently, the interaction of hnRNPK and ncRNAs was reported to play a critical role in gene regulation at transcriptional and post-transcriptional levels (15).

Long non-coding RNAs (lncRNAs) function as critical regulators of cancer metastasis, and their abnormal expression has been reported in many malignant tumors (16, 17). lncRNAs are known to govern many

cellular processes related to cancer malignancy partly by associating with various RBPs (18). Like mRNA, lncRNAs interdependently regulate gene expression by interacting with RBPs. Recently, several lncRNAs have been reported to directly interact with hnRNPK in the cytoplasm. c-Myc upregulated lncRNA (*MYU*) in colorectal cancer (CRC), was reported to directly interact with hnRNPK to stabilize the expression of cyclin-dependent kinase 6 (CDK6) (19). Several lncRNAs associated with hnRNPK including cancer susceptibility candidate 11 (*CASC11*) and Ets-1 promoter-associated noncoding RNA (*pancEts-1*) were reported to activate the Wnt pathway by stabilizing or activating b-catenin (20–22). Interaction of hnRNPK with *LINC01413* increases the expression of ZEB1 by inducing the nuclear translocation of YAP1/TAZ1 (22). In addition, *LINC00460* was identified as an hnRNPK-bound lincRNA in lung cancer cells. It potentiates the migratory and invasive abilities of lung cancer cells by inducing epithelial-mesenchymal transition (EMT) (23). Here, we found that *LINC00263* is a novel hnRNPK-regulated lincRNA and regulates malignant phenotypes. *LINC00263* is also called as oligodendrocyte maturation-associated long intergenic non-coding RNA (*OLMALINC*) and first reported to be more highly expressed in the white matter than in the gray matter of the human frontal cortex and to influence various genes that are associated with cytostructure, cell activation, and membrane signaling (24). *LINC00263* is also known to be upregulated in a wide range of cancer types including lung adenocarcinoma, colorectal cancer, and renal carcinoma (13). Consistent with our observation of its oncogenic potential, *LINC00263* was recently reported to be abnormally regulated in lung cancer (13).

Salmena et al. established the concept of ceRNA as a group of RNA transcripts that can quantitatively regulate miRNA through the sequence called MRE in ceRNA (10). Because miRNAs are partially complementary to the 3'UTR of the target mRNA, each miRNA has few hundreds of target genes; in other words, each mRNA can harbor multiple MREs. So far, several ncRNAs such as pseudogenes, antisense transcripts, and lncRNAs are reported to function as ceRNAs (25). As a ceRNA, lncRNAs compete with miRNAs for binding to their MRE in the endogenous target mRNA, thus causing a reduction and impairment of miRNA. For these reasons, ceRNAs are also termed as endogenous miRNA sponges. Several lncRNAs such as *MEG3* and *TUG1*, sequester multiple miRNAs from their target mRNA, thus leading to the derepression of target genes (26–29). Additionally, lncRNA *H19* harboring MREs for miR-138 and miR-200a, positively regulates the expression of *VIM*, *ZEB1/2*, and *TWIST2*, which are known EMT regulators. Therefore, lncRNA *H19* potentiates metastasis by abolishing the function of EMT-suppressing miRNAs (30, 31). In this study, ASO pull-down assays and small RNA sequencing revealed that several miRNAs interact strongly with *LINC00263*. Among them, miR-147a was selected as a putative decoy miRNA of *LINC00263*, which indicates that *LINC00263* controls the repressive function of miR-147a. Comparison of RNA sequencing data and miR-147a target genes revealed that CAPN2 is a downstream effector of hnRNPK/*LINC00263*/miR-147a. Mechanistically, *LINC00263* increases CAPN2 expression by functioning as a ceRNA of miR-147a, and thus potentiates malignant capabilities. CAPN2 is a calcium-dependent protease that is highly upregulated in various cancers (32). CAPN2 is known to play an important role in proliferation and metastasis of cancer cells (33), and it was also reported to function as an oncogene by inducing EMT and increasing expression of matrix metalloproteinase 9 (*MMP9*) (32, 34). Abnormal expression of CAPN2 is closely associated with poor prognosis of ovarian

cancer patients (35) and is related to metastatic prostate cancer by potentiating proliferative and invasive capabilities (36, 37).

Conclusion

Based on our findings, the regulatory role of hnRNPK/*LINC00263*/miR-147a/CAPN2 in cancer malignancy is schematically summarized in Fig. 8. Briefly, *LINC00263* is regulated by hnRNPK and functions as a ceRNA for *CAPN2*-targeting miR-147a. Under conditions of high hnRNPK, *LINC00263* is highly expressed thereby reducing the amount of *CAPN2*-targeting miR-147a. Increased CAPN2 promotes the malignant phenotypes including invasiveness, proliferation, and clonogenicity. Conversely, low hnRNPK results in the decreased *LINC00263*, which potentiates miR-147a-mediated suppression of CAPN2. Therefore, the malignant capabilities are diminished. Taken together, our data suggest that hnRNPK/*LINC00263*/miR-147a/CAPN2 represents a promising target for the development of cancer therapeutics.

Abbreviations

hnRNPK, heterogeneous nuclear ribonucleoprotein K; lincRNA, long intergenic non-coding RNA; miRNA, microRNA; ceRNA, competitive endogenous RNA; UTR, untranslated region; RNP-IP, ribonucleoprotein immunoprecipitation; ASO-PD, antisense oligonucleotide pull-down.

Declarations

Ethics approval and consent to participate

Not applicable

Consent for publication

Not applicable

Availability of data and materials

The datasets used and/or analysed during the current study are available from the corresponding author on reasonable request.

Competing interests

The authors declare that they have no conflict of interest.

Funding

This study was supported by a grant from the Mid-career Research Program (HHK, NRF-2017R1A2A2A05069691) and the Basic Research Program (HHK, NRF-2020R1F1A1068888), through the

National Research Foundation (NRF) funded by Ministry of Science and ICT, and Global PH.D Fellowship Program (WJL, NRF-2017H1A2A1045644) through the National Research Foundation of Korea(NRF) funded by the Ministry of Education.

Authors' contributions

WJL participates in formulating the concepts and designs of study, performing the experiments, and analyzing/interpretating the experimental data; CHS participates in performing the experiments; HJ participates in performing the experiments; SDJ participates in performing the experiments; MSP participates in analyzing/interpretating the bioinformatic data; HHW participates in interpretating the bioinformatic data; PRP participates in performing the experiments; MG participates in analyzing/interpretating the experimental data; HHK participates in formulating the concepts and designs of study, analyzing/interpretating the experimental data, writing the manuscript, and acquiring the fund. All authors read and approved the final manuscript.

Acknowledgements

PRP and MG were supported by the NIA IRP, NIH.

References

1. Demicheli R, Dillekas H, Straume O, Biganzoli E. Distant metastasis dynamics following subsequent surgeries after primary breast cancer removal. Breast Cancer Res. 2019;21(1):57.
2. Feitelson MA, Arzumanyan A, Kulathinal RJ, Blain SW, Holcombe RF, Mahajna J, et al. Sustained proliferation in cancer: Mechanisms and novel therapeutic targets. Semin Cancer Biol. 2015;35 Suppl:S25-S54.
3. Zhuang X, Zhang H, Hu G. Cancer and Microenvironment Plasticity: Double-Edged Swords in Metastasis. Trends Pharmacol Sci. 2019;40(6):419-29.
4. Siomi H, Matunis MJ, Michael WM, Dreyfuss G. The pre-mRNA binding K protein contains a novel evolutionarily conserved motif. Nucleic Acids Res. 1993;21(5):1193-8.
5. Gao R, Yu Y, Inoue A, Widodo N, Kaul SC, Wadhwa R. Heterogeneous nuclear ribonucleoprotein K (hnRNP-K) promotes tumor metastasis by induction of genes involved in extracellular matrix, cell movement, and angiogenesis. J Biol Chem. 2013;288(21):15046-56.
6. Chung IC, Chen LC, Chung AK, Chao M, Huang HY, Hsueh C, et al. Matrix metalloproteinase 12 is induced by heterogeneous nuclear ribonucleoprotein K and promotes migration and invasion in nasopharyngeal carcinoma. BMC Cancer. 2014;14:348.
7. Inoue A, Sawata SY, Taira K, Wadhwa R. Loss-of-function screening by randomized intracellular antibodies: identification of hnRNP-K as a potential target for metastasis. Proc Natl Acad Sci U S A. 2007;104(21):8983-8.

8. Shin CH, Lee H, Kim HR, Choi KH, Joung JG, Kim HH. Regulation of PLK1 through competition between hnRNPK, miR-149-3p and miR-193b-5p. Cell Death Differ. 2017;24(11):1861-71.
9. Shin CH, Ryu S, Kim HH. hnRNPK-regulated PTOV1-AS1 modulates heme oxygenase-1 expression via miR-1207-5p. BMB Rep. 2017;50(4):220-5.
10. Salmena L, Poliseno L, Tay Y, Kats L, Pandolfi PP. A ceRNA hypothesis: the Rosetta Stone of a hidden RNA language? Cell. 2011;146(3):353-8.
11. Cao MX, Jiang YP, Tang YL, Liang XH. The crosstalk between lncRNA and microRNA in cancer metastasis: orchestrating the epithelial-mesenchymal plasticity. Oncotarget. 2017;8(7):12472-83.
12. Yuan JH, Yang F, Wang F, Ma JZ, Guo YJ, Tao QF, et al. A long noncoding RNA activated by TGF-beta promotes the invasion-metastasis cascade in hepatocellular carcinoma. Cancer Cell. 2014;25(5):666-81.
13. Liu S, Lai W, Shi Y, Liu N, Ouyang L, Zhang Z, et al. Annotation and cluster analysis of long noncoding RNA linked to male sex and estrogen in cancers. NPJ Precis Oncol. 2020;4:5.
14. Wang Z, Qiu H, He J, Liu L, Xue W, Fox A, et al. The emerging roles of hnRNPK. J Cell Physiol. 2020;235(3):1995-2008.
15. Xu Y, Wu W, Han Q, Wang Y, Li C, Zhang P, et al. New Insights into the Interplay between Non-Coding RNAs and RNA-Binding Protein HnRNPK in Regulating Cellular Functions. Cells. 2019;8(1).
16. Xu Q, Deng F, Qin Y, Zhao Z, Wu Z, Xing Z, et al. Long non-coding RNA regulation of epithelial-mesenchymal transition in cancer metastasis. Cell Death Dis. 2016;7(6):e2254.
17. Dhamija S, Diederichs S. From junk to master regulators of invasion: lncRNA functions in migration, EMT and metastasis. Int J Cancer. 2016;139(2):269-80.
18. Dangelmaier E, Lal A. Adaptor proteins in long noncoding RNA biology. Biochim Biophys Acta Gene Regul Mech. 2020;1863(4):194370.
19. Kawasaki Y, Komiya M, Matsumura K, Negishi L, Suda S, Okuno M, et al. MYU, a Target lncRNA for Wnt/c-Myc Signaling, Mediates Induction of CDK6 to Promote Cell Cycle Progression. Cell Rep. 2016;16(10):2554-64.
20. Zhang Z, Zhou C, Chang Y, Zhang Z, Hu Y, Zhang F, et al. Long non-coding RNA CASC11 interacts with hnRNP-K and activates the WNT/beta-catenin pathway to promote growth and metastasis in colorectal cancer. Cancer Lett. 2016;376(1):62-73.
21. Li D, Wang X, Mei H, Fang E, Ye L, Song H, et al. Long Noncoding RNA pancEts-1 Promotes Neuroblastoma Progression through hnRNPK-Mediated beta-Catenin Stabilization. Cancer Res. 2018;78(5):1169-83.
22. Ji L, Li X, Zhou Z, Zheng Z, Jin L, Jiang F. LINC01413/hnRNP-K/ZEB1 Axis Accelerates Cell Proliferation and EMT in Colorectal Cancer via Inducing YAP1/TAZ1 Translocation. Mol Ther Nucleic Acids. 2020;19:546-61.
23. Li K, Sun D, Gou Q, Ke X, Gong Y, Zuo Y, et al. Long non-coding RNA linc00460 promotes epithelial-mesenchymal transition and cell migration in lung cancer cells. Cancer Lett. 2018;420:80-90.

24. Mills JD, Kavanagh T, Kim WS, Chen BJ, Waters PD, Halliday GM, et al. High expression of long intervening non-coding RNA OLMALINC in the human cortical white matter is associated with regulation of oligodendrocyte maturation. Mol Brain. 2015;8:2.
25. Karreth FA, Pandolfi PP. ceRNA cross-talk in cancer: when ce-bling rivalries go awry. Cancer Discov. 2013;3(10):1113-21.
26. Moradi MT, Fallahi H, Rahimi Z. Interaction of long noncoding RNA MEG3 with miRNAs: A reciprocal regulation. J Cell Biochem. 2019;120(3):3339-52.
27. Peng W, Si S, Zhang Q, Li C, Zhao F, Wang F, et al. Long non-coding RNA MEG3 functions as a competing endogenous RNA to regulate gastric cancer progression. J Exp Clin Cancer Res. 2015;34:79.
28. Zhou H, Sun L, Wan F. Molecular mechanisms of TUG1 in the proliferation, apoptosis, migration and invasion of cancer cells. Oncol Lett. 2019;18(5):4393-402.
29. Tang T, Cheng Y, She Q, Jiang Y, Chen Y, Yang W, et al. Long non-coding RNA TUG1 sponges miR-197 to enhance cisplatin sensitivity in triple negative breast cancer. Biomed Pharmacother. 2018;107:338-46.
30. Liang WC, Fu WM, Wong CW, Wang Y, Wang WM, Hu GX, et al. The lncRNA H19 promotes epithelial to mesenchymal transition by functioning as miRNA sponges in colorectal cancer. Oncotarget. 2015;6(26):22513-25.
31. Yang Q, Wang X, Tang C, Chen X, He J. H19 promotes the migration and invasion of colon cancer by sponging miR-138 to upregulate the expression of HMGA1. Int J Oncol. 2017;50(5):1801-9.
32. Miao C, Liang C, Tian Y, Xu A, Zhu J, Zhao K, et al. Overexpression of CAPN2 promotes cell metastasis and proliferation via AKT/mTOR signaling in renal cell carcinoma. Oncotarget. 2017;8(58):97811-21.
33. Li P, Miao C, Liang C, Shao P, Wang Z, Li J. Silencing CAPN2 Expression Inhibited Castration-Resistant Prostate Cancer Cells Proliferation and Invasion via AKT/mTOR Signal Pathway. Biomed Res Int. 2017;2017:2593674.
34. Chen B, Tang J, Guo YS, Li Y, Chen ZN, Jiang JL. Calpains are required for invasive and metastatic potentials of human HCC cells. Cell Biol Int. 2013;37(7):643-52.
35. Storr SJ, Safuan S, Woolston CM, Abdel-Fatah T, Deen S, Chan SY, et al. Calpain-2 expression is associated with response to platinum based chemotherapy, progression-free and overall survival in ovarian cancer. J Cell Mol Med. 2012;16(10):2422-8.
36. Rios-Doria J, Kuefer R, Ethier SP, Day ML. Cleavage of beta-catenin by calpain in prostate and mammary tumor cells. Cancer Res. 2004;64(20):7237-40.
37. Rios-Doria J, Day KC, Kuefer R, Rashid MG, Chinnaiyan AM, Rubin MA, et al. The role of calpain in the proteolytic cleavage of E-cadherin in prostate and mammary epithelial cells. J Biol Chem. 2003;278(2):1372-9.

Supplementary Information

Additional file contains supplementary information including 10 figures and 3 tables.

Supplementary fig. 1 Analyses of RNA sequencing data. (**a**-**b**) Various analyses plots, including scatter, volcano, and volume plots were generated corresponding to the RNA sequencing data obtained from hnRNPK- (**a**) and *LINC00263*-silenced HeLa cells (**b**). Gene ontology (GO) analyses are also shown (**c**).

Supplementary fig. 2 Interaction of hnRNPK with *LINC00263* is dependent on KH1 and KH2 domains. (**a**-**b**) Prediction of hnRNPK binding sites in LINC00263 using RBPmap (http://rbpmap.technion.ac.il/) was shown (**a**). Each binding locations and sequences were also presented (**b**).

Supplementary fig. 3 Verification of overexpression and knockdown by RT-qPCR or Western blot analyses. (**a**) Following the transfection of HeLa cells with overexpression vector (pcDNA/*LINC00263*), the expression of *LINC00263* was assessed by RT-qPCR analysis. (**b**-**c**) miR-147a overexpression by pre-miR-147a (**b**) and inhibition by anti-miR-147a (**c**) were verified by RT-qPCR analysis using miRNA-specific TaqMan primer. (**d**) To determine the efficiency of CAPN2 overexpression vector, HeLa cells were transfected with various concentrations of the vector and the level of CAPN2 was determined by Western blot analysis. For the rescue experiments, 4 mg of vector was used.

Supplementary fig. 4 Identification of *LINC00263*-associated miRNAs by antisense oligonucleotide pull-down (ASO PD) followed by small RNA sequencing. (**a**) Schematic of the ASO PD experiment and the sequences of *LacZ* and *LINC00263* ASOs used in this study. (**b**) Volcano plot of small RNA sequencing and 24 miRNAs enriched in *LINC00263* ASO PD that were selected as putative decoy targets of *LINC00263* are shown. (**c**) Using a bioinformatic tool (RNA22, https://cm.jefferson.edu/rna22/Interactive), four of the 24 miRNAs were predicted to strongly interact with *LINC00263*. Among them, miR-147a was selected for further studies based on its folding energy and significance.

Supplementary fig. 5 Three individual results of RNP-IP experiments. All RNP-IP results indicate the mean and standard deviation of the values obtained in three independent experiments. (**a**) *LINC00263* in Ago2 RNP-IP; (**b**) *LINC00263* in Ago2 RNP-IP with high expression of miR-147a; (**c**) *CAPN2* mRNA in Ago2 RNP-IP; (**d**-**e**) *CAPN2* mRNA in Ago2 RNP-IP with high (**d**) and low expression (**e**) of miR-147a; (**f**) *CAPN2* mRNA in Ago2 RNP-IP with knockdown of hnRNPK or *LINC00263*; (**g**) *CAPN2* mRNA in Ago2 RNP-IP in rescue experiments.

Supplementary fig. 6 The levels of common target genes in hnRNPK- and *LINC00263*-silenced cells. To test whether knockdown of hnRNPK and *LINC00263* decreased the expression of miR-147a target genes, the levels of common target mRNAs were examined by RT-qPCR analysis.

Supplementary fig. 7 Schematic of the luciferase reporter vectors containing wild-type or mutant sequences of miR-147a MRE. (**a**-**b**) Luciferase reporter vectors (wild-type and mutant) with miR-147a MREs in *LINC00263* sequence. Using bioinformatic tools, two MREs were identified in the *LINC00263*

sequence: miR-147a binding site #1 and #2. (**c**) Luciferase reporter vectors (wild-type and mutant) with miR-147a MRE in the 3'UTR of *CAPN2* mRNA.

Supplementary fig. 8 Search for intracellular signaling molecules linked to hnRNPK/*LINC00263*. To identify the signaling molecules, the activation of which is involved in the oncogenic function of hnRNPK/*LINC00263*, the Proteome Profiler Human Phospho-Kinase Array Kit (R&D Systems, ARY003B) was used. Briefly, HeLa cells were transfected with *HNRNPK* or *LINC00263* siRNA and whole cell lysates were incubated with each array in which various capture antibodies were spotted. Phosphorylated signaling molecules were detected by incubating with biotinylated phospho-specific detection antibodies and then visualized using chemiluminescent reagents. (**a**) Total results of the Proteome Profiler Human Phospho-Kinase Array. (**b**) Selected spots that were decreased in the hnRNPK- and *LINC00263*-silenced cells: p-ERK and p-p70S6K. (**c**) HeLa cells were transfected with control siRNA, *HNRNPK* siRNA, *LINC00263* siRNA, pre-miR-147a, or *CAPN2* siRNA. Following preparation of whole cell lysates, Western blot analysis was performed using the indicated antibodies. The level of GAPDH protein served as a loading control.

Supplementary fig. 9 Comparison of *LINC00263* expression level in lung cancer patients. (**a**-**b**) The expression of *LINC00263* was compared between non-malignant and non-small cell lung cancer tissues (**a**, GSE81089), or normal and tumor tissues (**b**, GSE40419). (**c**) The invasive ability of two lung cancer cells was assessed by Transwell invasion assay. (**d**) Invasiveness of *LINC00263*-overexpressing H460 cells was determined by comparing the number of invading cells. Bars on microscopic images represent 100 mm. Statistical analyses were performed using the Student's *t*-test using three independent experiments (* $p < 0.05$). All data represent mean ± standard variation (SD).

Supplementary fig. 10 Uncropped Western blot images shown in this manuscript.

Supplementary table 1 Sequences of small interfering RNAs (siRNAs) used in this study.

Supplementary table 2 Information about the antibodies used in this study.

Supplementary table 3 Sequences of the RT-qPCR primers used in this study.

Figures

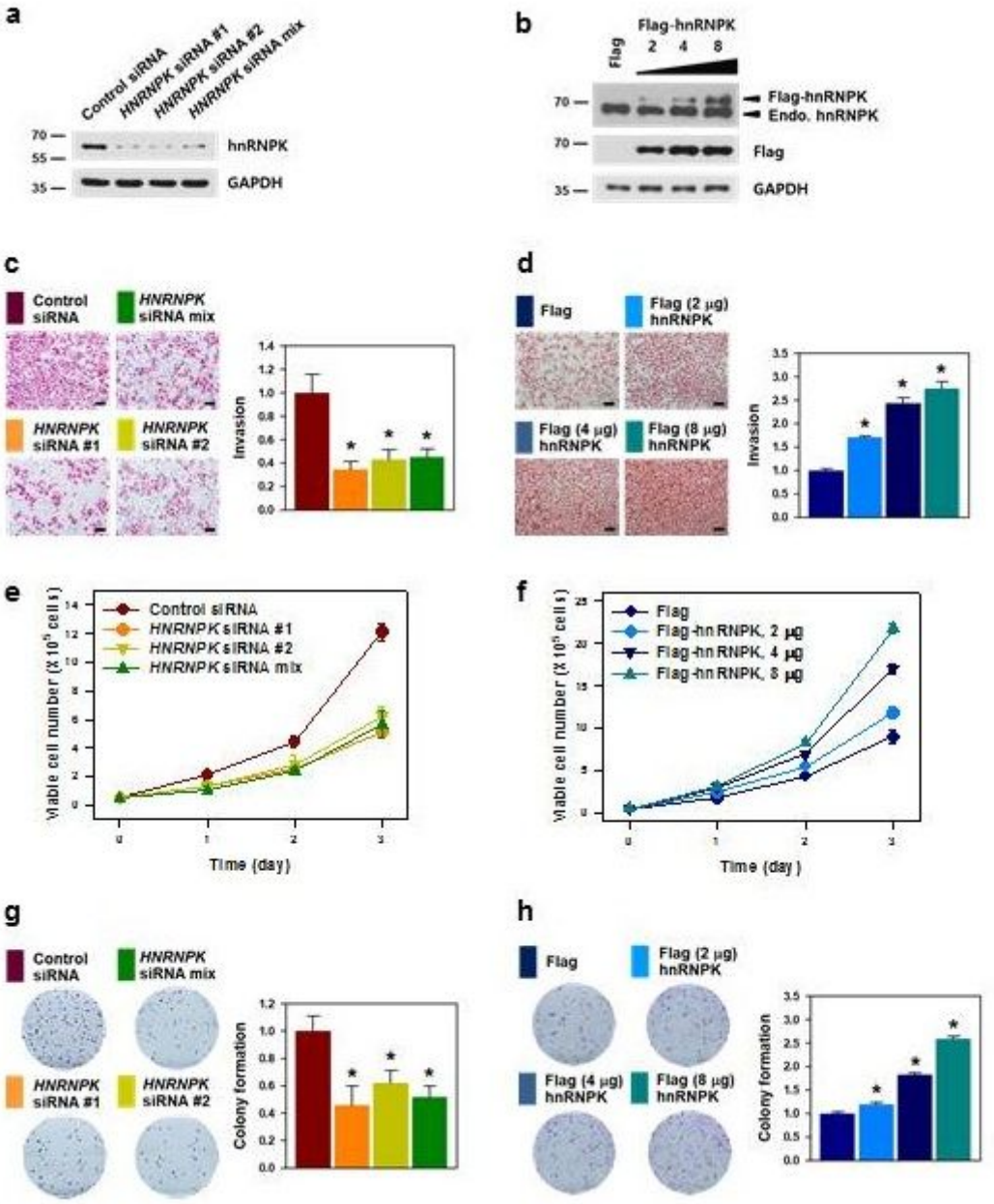

Figure 1

hnRNPK is responsible for the cancer malignancy. To investigate the role of hnRNPK in malignant phenotype, two individual and mixed HNRNPK siRNAs were transfected into HeLa cells (a, c, e, and g). In contrast, Flag-hnRNPK vector was constructed and used for hnRNPK overexpression (b, d, f, and h). (a-b) The efficiency of hnRNPK knockdown (a), and overexpression (b) was determined by analyzing the level of hnRNPK by Western blot analysis. (c-d) Invasive ability was assessed by Transwell invasion assay in vitro. Representative images of the invaded cells are shown. Invasiveness was determined by counting the number of invaded cells from more than ten fields. (e-f) To determine the proliferation rate, equal number of transfected HeLa cells were plated in 12-well plates and the number of viable cells was counted under a microscope at the indicated times. (g-h) Equal number of transfected cells were plated in

6-well plates, and clonogenicity was determined by counting the number of colonies. Bars on microscopic images represent 100 μm. Statistical analyses were performed using the Student's t-test using three independent experiments (* $p < 0.05$). All data represent mean ± standard variation (SD).

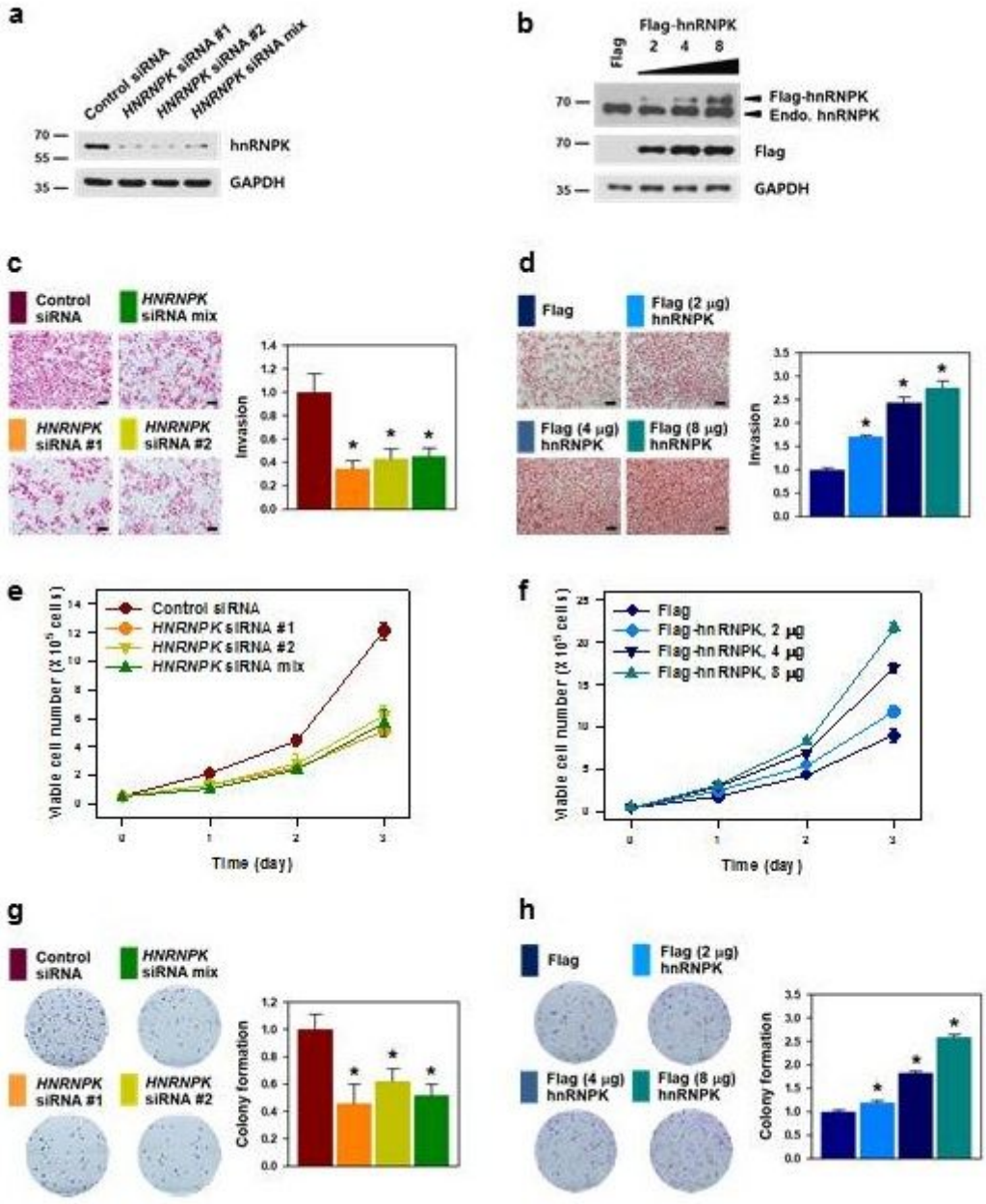

Figure 1

hnRNPK is responsible for the cancer malignancy. To investigate the role of hnRNPK in malignant phenotype, two individual and mixed HNRNPK siRNAs were transfected into HeLa cells (a, c, e, and g). In contrast, Flag-hnRNPK vector was constructed and used for hnRNPK overexpression (b, d, f, and h). (a-b) The efficiency of hnRNPK knockdown (a), and overexpression (b) was determined by analyzing the level of hnRNPK by Western blot analysis. (c-d) Invasive ability was assessed by Transwell invasion assay in vitro. Representative images of the invaded cells are shown. Invasiveness was determined by counting

the number of invaded cells from more than ten fields. (e-f) To determine the proliferation rate, equal number of transfected HeLa cells were plated in 12-well plates and the number of viable cells was counted under a microscope at the indicated times. (g-h) Equal number of transfected cells were plated in 6-well plates, and clonogenicity was determined by counting the number of colonies. Bars on microscopic images represent 100 μm. Statistical analyses were performed using the Student's t-test using three independent experiments (* $p < 0.05$). All data represent mean ± standard variation (SD).

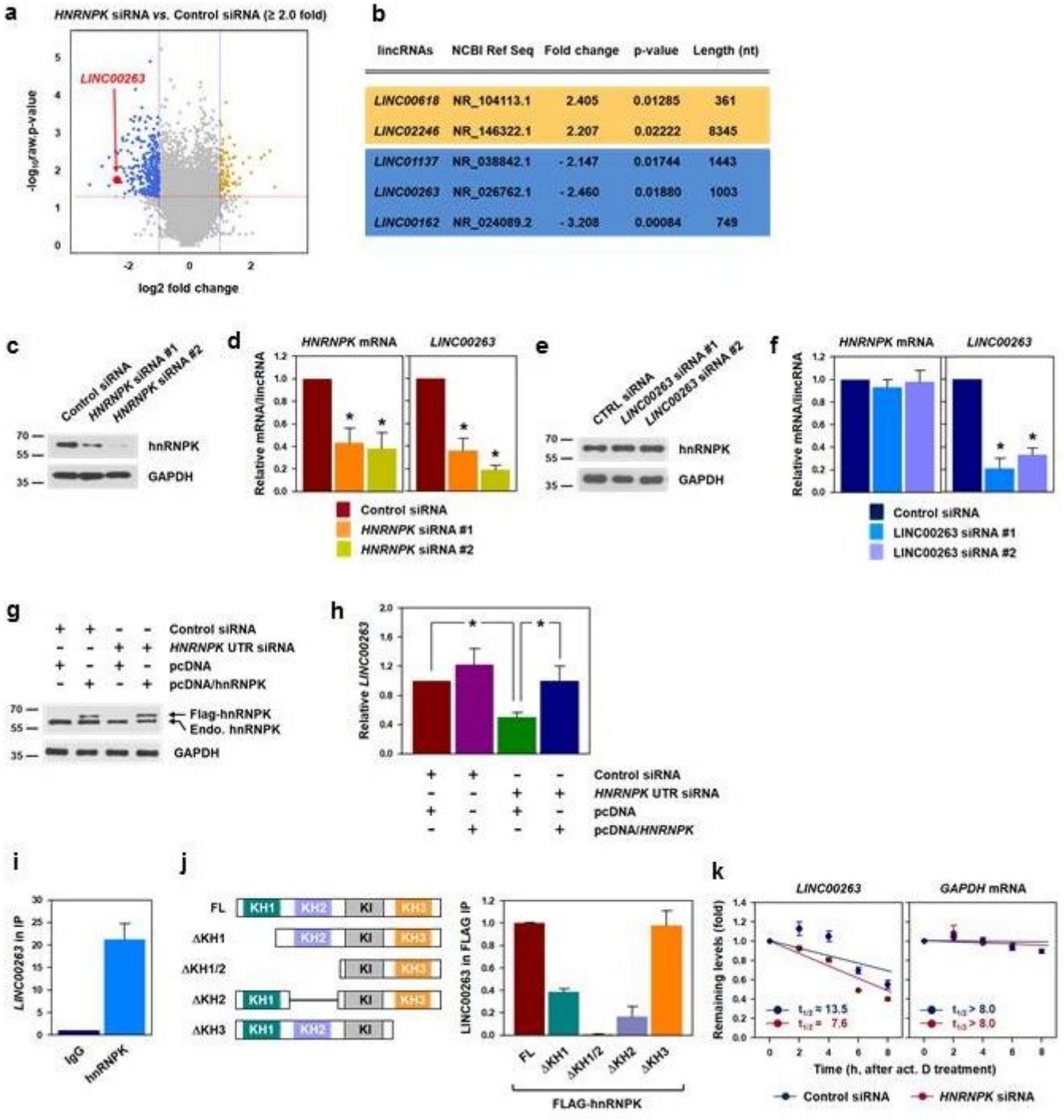

Figure 2

LINC00263 is a novel target of hnRNPK. (a-b) To identify hnRNPK-regulated lincRNAs, RNA sequencing was performed using total RNAs isolated from hnRNPK- and LINC00263-silenced HeLa cells. (a) Volcano plots were generated by analyzing the sequencing data. (b) Information about the five hnRNPK-regulated lincRNAs is summarized. (c-d) RNA sequencing results were verified by assessing the level of LINC00263 in hnRNPK-silenced cells. Knockdown of hnRNPK by two independent siRNAs was verified by Western blot analysis (c) and the levels of HNRNPK mRNA and LINC00263 were determined by RT-qPCR analysis (d). To check whether knockdown of LINC00263 affects hnRNPK expression, the levels of hnRNPK protein (e) and HNRNPK mRNA (f) were determined by Western blot and RT-qPCR analyses, respectively. (g-h) To confirm that hnRNPK regulates LINC00263, a specific siRNA targeting the 3'UTR of HNRNPK mRNA was used. HeLa cells were cotransfected with the 3'UTR-specific HNRNPK siRNAs and Flag-hnRNPK vector. The level of endogenous and ectopic hnRNPK (Flag-hnRNPK) was determined by Western blot analysis. GAPDH was used as a loading control (g). The level of LINC00263 in transfected cells as described above were determined by RT-qPCR analysis (h). (i) Direct association of hnRNPK with LINC00263 was tested by RNP-IP experiment using control IgG and hnRNPK antibody. The enrichment of LINC00263 was calculated by comparing the level of LINC00263 in IgG and hnRNPK IP materials. The level of LINC00263 was determined by RT-qPCR analysis and 18S was used for normalization. (j) Following transfection of HeLa cells with wild-type (full length, FL) or four deletion mutant vectors, RNP-IP was performed using an anti-Flag antibody. The level of LINC00263 in the Flag IP was quantified by RT-qPCR analysis. Schematic represents wild-type and four mutants of hnRNPK (ΔKH1, ΔKH1/2, ΔKH2, and ΔKH3) used in this study. (k) The effect of hnRNPK on the stability of LINC00263 was examined. Following treatment of actinomycin D (0.5 μg/ml), cells were harvested at the indicated times and the levels of LINC00263 and GAPDH mRNA were determined by RT-qPCR analysis. Statistical analyses were performed using the Student’s t-test using three independent experiments (* $p < 0.05$). All data represent mean ± standard variation (SD).

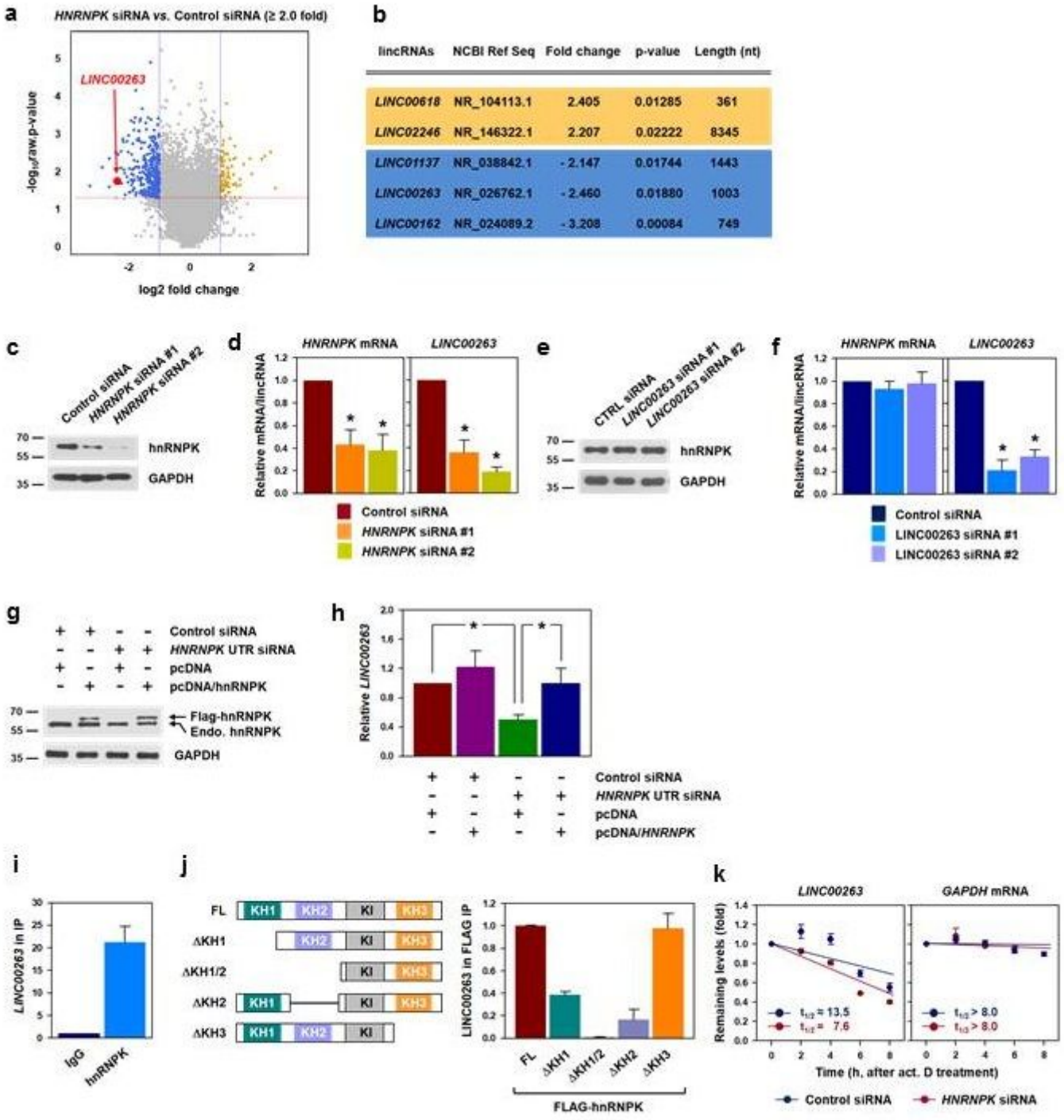

Figure 2

LINC00263 is a novel target of hnRNPK. (a-b) To identify hnRNPK-regulated lincRNAs, RNA sequencing was performed using total RNAs isolated from hnRNPK- and LINC00263-silenced HeLa cells. (a) Volcano plots were generated by analyzing the sequencing data. (b) Information about the five hnRNPK-regulated lincRNAs is summarized. (c-d) RNA sequencing results were verified by assessing the level of LINC00263 in hnRNPK-silenced cells. Knockdown of hnRNPK by two independent siRNAs was verified by Western blot analysis (c) and the levels of HNRNPK mRNA and LINC00263 were determined by RT-qPCR analysis

(d). To check whether knockdown of LINC00263 affects hnRNPK expression, the levels of hnRNPK protein (e) and HNRNPK mRNA (f) were determined by Western blot and RT-qPCR analyses, respectively. (g-h) To confirm that hnRNPK regulates LINC00263, a specific siRNA targeting the 3'UTR of HNRNPK mRNA was used. HeLa cells were cotransfected with the 3'UTR-specific HNRNPK siRNAs and Flag-hnRNPK vector. The level of endogenous and ectopic hnRNPK (Flag-hnRNPK) was determined by Western blot analysis. GAPDH was used as a loading control (g). The level of LINC00263 in transfected cells as described above were determined by RT-qPCR analysis (h). (i) Direct association of hnRNPK with LINC00263 was tested by RNP-IP experiment using control IgG and hnRNPK antibody. The enrichment of LINC00263 was calculated by comparing the level of LINC00263 in IgG and hnRNPK IP materials. The level of LINC00263 was determined by RT-qPCR analysis and 18S was used for normalization. (j) Following transfection of HeLa cells with wild-type (full length, FL) or four deletion mutant vectors, RNP-IP was performed using an anti-Flag antibody. The level of LINC00263 in the Flag IP was quantified by RT-qPCR analysis. Schematic represents wild-type and four mutants of hnRNPK (ΔKH1, ΔKH1/2, ΔKH2, and ΔKH3) used in this study. (k) The effect of hnRNPK on the stability of LINC00263 was examined. Following treatment of actinomycin D (0.5 μg/ml), cells were harvested at the indicated times and the levels of LINC00263 and GAPDH mRNA were determined by RT-qPCR analysis. Statistical analyses were performed using the Student's t-test using three independent experiments (* $p < 0.05$). All data represent mean ± standard variation (SD).

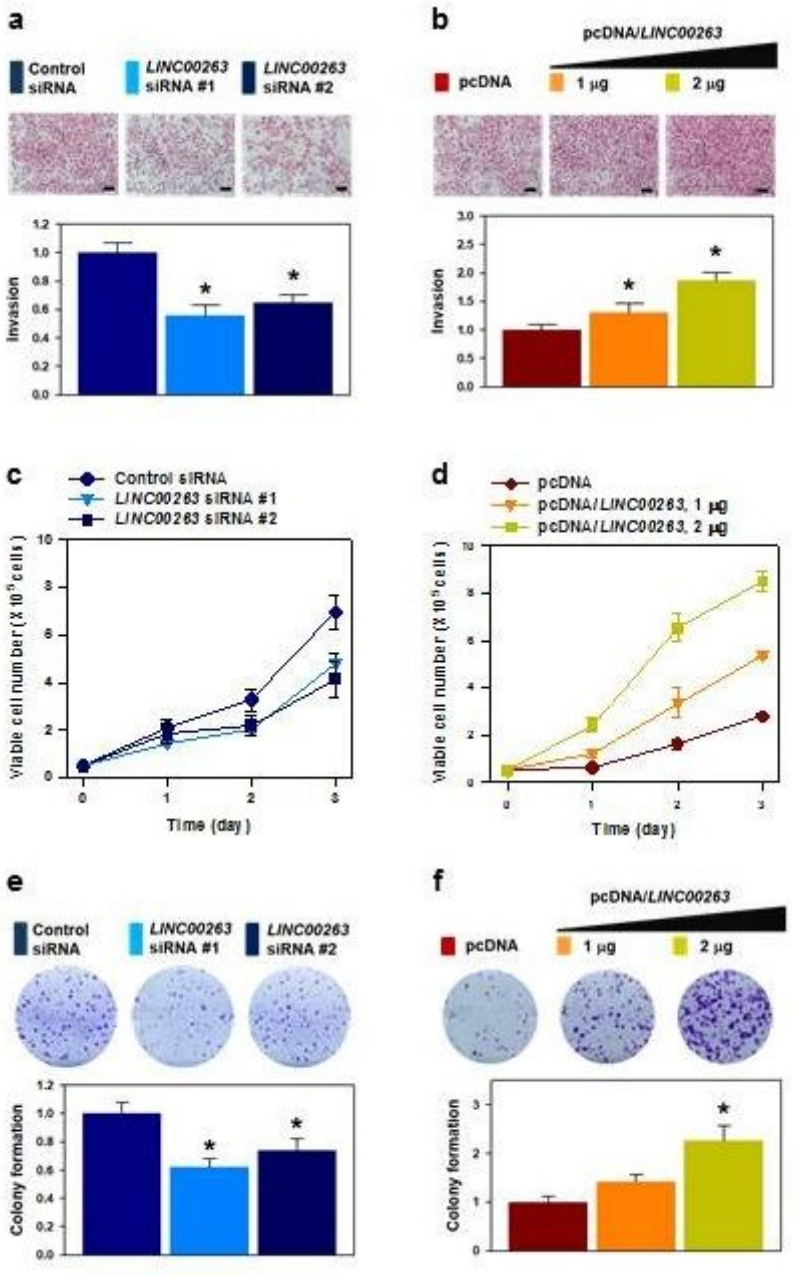

Figure 3

LINC00263 regulates the malignant phenotypes. To investigate whether LINC00263 is required for hnRNPK-mediated malignant phenotypes, two independent siRNAs (a, c, and e) and overexpression vector (pcDNA/LINC00263: b, d, and f) were used. Invasiveness was determined using Transwell invasion assay (a-b). Cellular proliferation (c-d) and clonogenicity (e-f) were assessed by counting the number of viable cells and colonies, respectively, as described in Materials and methods. Bars on microscopic images represent 100 μm. Statistical analyses were performed using the Student's t-test using three independent experiments (* $p < 0.05$). All data represent mean ± standard variation (SD).

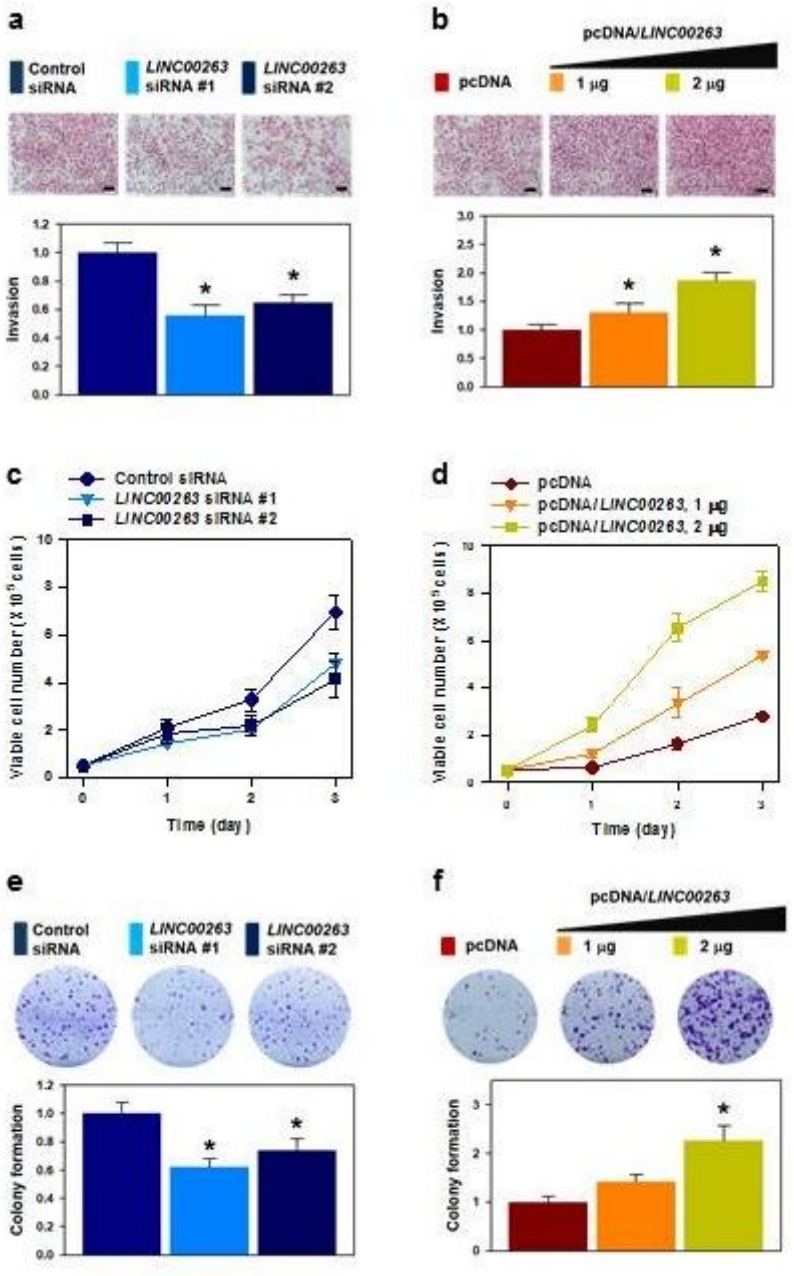

Figure 3

LINC00263 regulates the malignant phenotypes. To investigate whether LINC00263 is required for hnRNPK-mediated malignant phenotypes, two independent siRNAs (a, c, and e) and overexpression vector (pcDNA/LINC00263: b, d, and f) were used. Invasiveness was determined using Transwell invasion assay (a-b). Cellular proliferation (c-d) and clonogenicity (e-f) were assessed by counting the number of viable cells and colonies, respectively, as described in Materials and methods. Bars on microscopic images represent 100 μm. Statistical analyses were performed using the Student's t-test using three independent experiments (* $p < 0.05$). All data represent mean ± standard variation (SD).

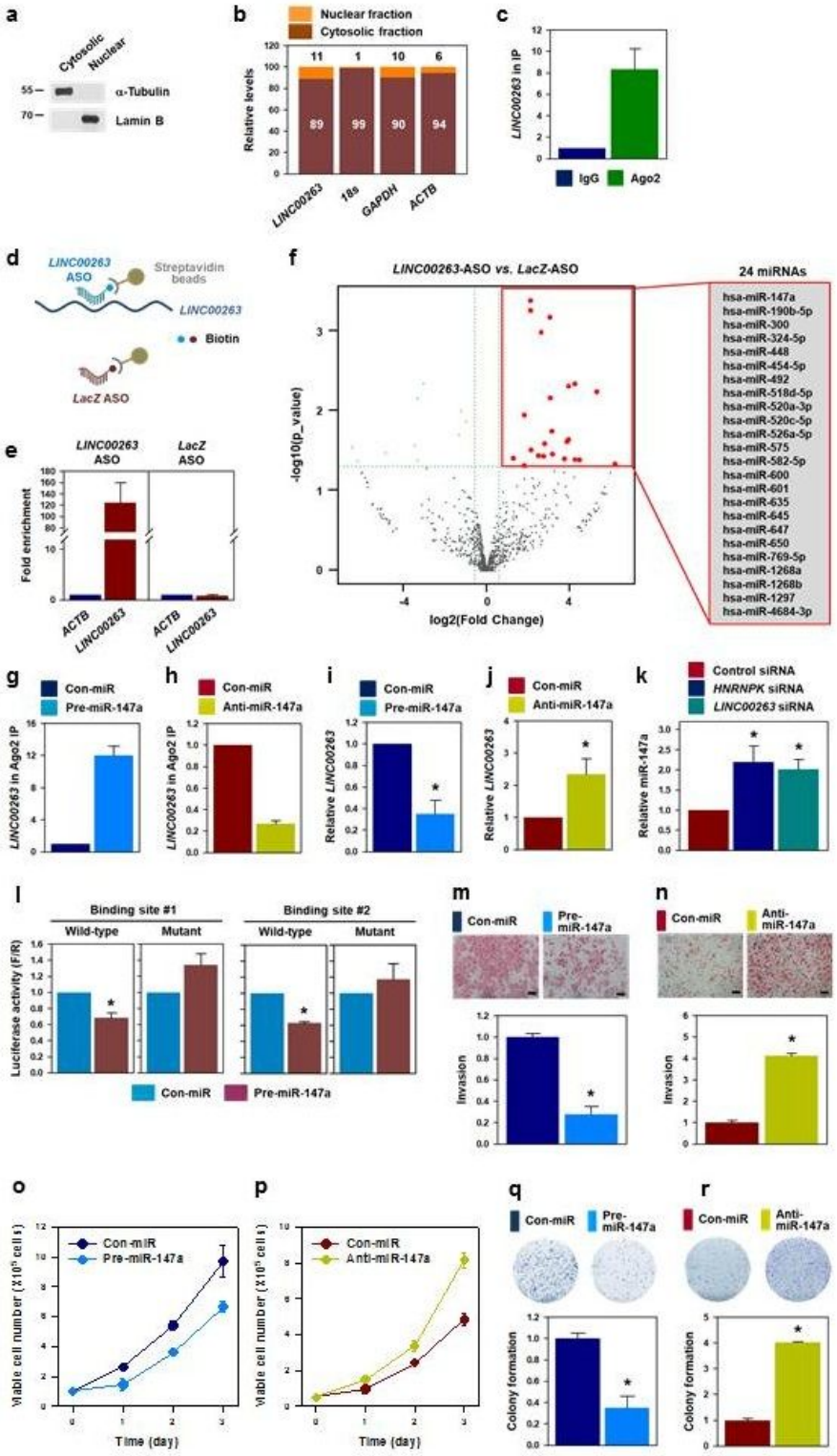

Figure 4

LINC00263 functions as ceRNA for miR-147a. (a-b) Cellular fractionation assay was performed to check the localization of LINC00263. To ensure the purity of the fractions, the levels of α-tubulin (cytosolic marker) and lamin B (nuclear marker) were analyzed by Western blot analysis (a). The levels of LINC00263, 18S, GAPDH, and ACTB mRNA in each fraction were determined by RT-qPCR analysis (b). (c) To check whether LINC00263 is involved in miRISC, Ago2 RNP-IP was performed using specific antibody.

The level of LINC00263 in control IgG and Ago2 IP materials was determined by RT-qPCR analysis and normalized to the level of GAPDH mRNA. (d-f) To screen for LINC00263-associated miRNAs, antisense oligonucleotide pull-down (ASO PD) was performed. Schematic of the experimental design is shown (d). Detailed information of the ASO sequences for LacZ (control) and LINC00263 was provided into Supplementary fig. 4a. Efficiency of ASO PD was examined by comparing the level of LINC00263 in ASO PD materials (e). Small RNA sequencing was performed with RNAs isolated from ASO PD materials. miRNAs with higher expression in LINC00263 ASO PD are listed (f and Supplementary fig. 4b). (g-j) HeLa cells were transfected with pre-miR-147a (for overexpression, g and i) or anti-miR-147a (for inhibition, h and j). Direct association of LINC00263 with miR-147a-involved miRISC was analyzed by Ago2 RNP-IP (g-h) and the level of LINC00263 was determined by RT-qPCR analysis (i-j). (k) Following knockdown of hnRNPK and LINC00263, the level of miR-147a was determined by RT-qPCR analysis. (l) Bioinformatic analyses revealed that two MREs of miR-147a exist in LINC00263 sequence (Supplementary fig. 7a and 7b). To examine the sequence-specific interaction, luciferase reporter vectors containing wild-type or mutant sequences of miR-147a MREs were constructed. Following overexpression of miR-147a, the luciferase activity was assessed as described in Materials and methods. (m-r) To investigate the effect of miR-147a on malignant capabilities, pre-miR-147a (m, o, and q) or anti-miR-147a (n, p, and r) were introduced into HeLa cells. Malignant phenotypes including invasiveness (m-n), proliferation rate (o-p), and clonogenicity (q-r) were examined as described in Materials and methods. Bars on microscopic images represent 100 μm. Statistical analyses were performed using the Student’s t-test using three independent experiments (* $p < 0.05$). All data represent mean ± standard variation (SD).

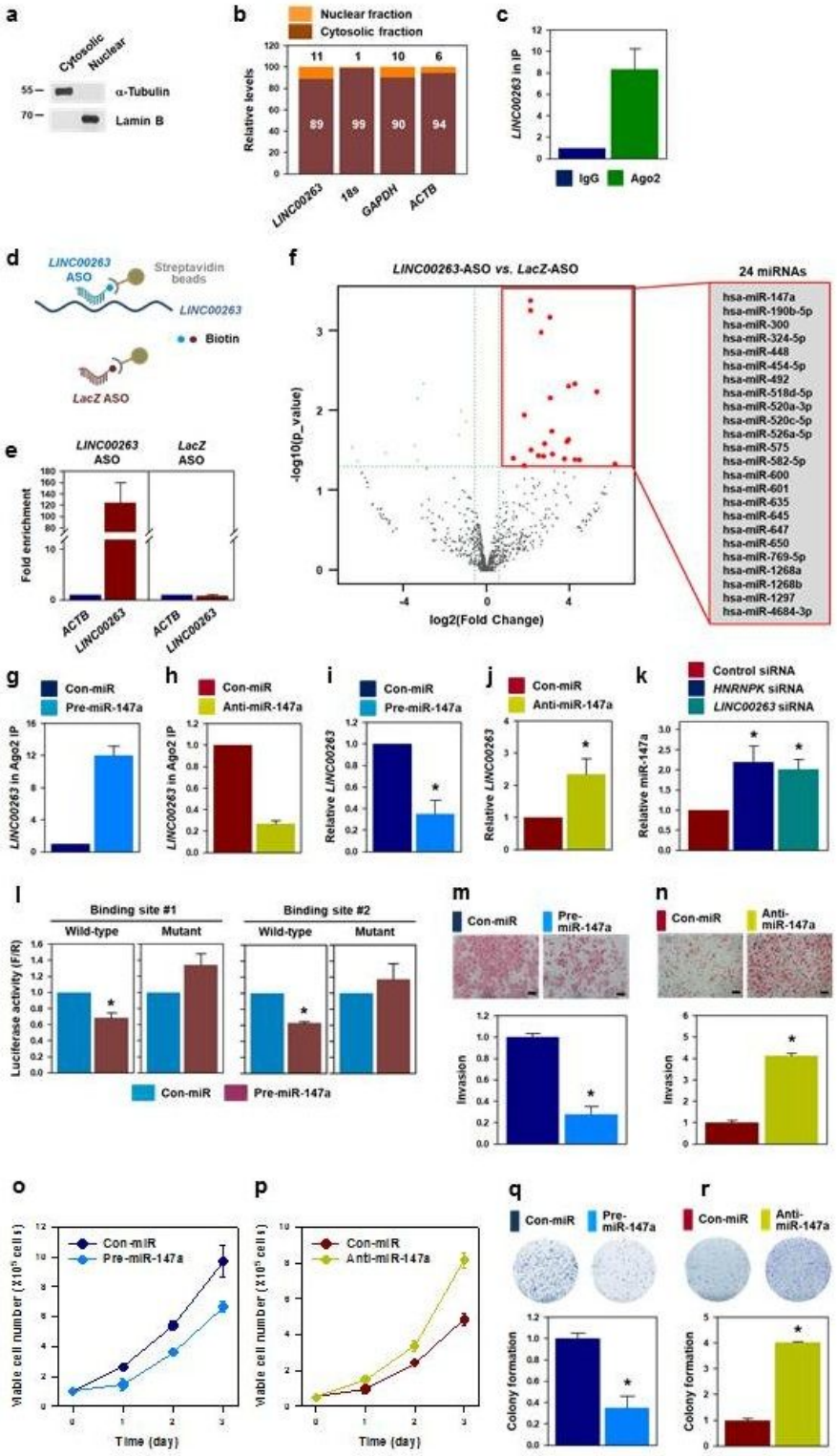

Figure 4

LINC00263 functions as ceRNA for miR-147a. (a-b) Cellular fractionation assay was performed to check the localization of LINC00263. To ensure the purity of the fractions, the levels of α-tubulin (cytosolic marker) and lamin B (nuclear marker) were analyzed by Western blot analysis (a). The levels of LINC00263, 18S, GAPDH, and ACTB mRNA in each fraction were determined by RT-qPCR analysis (b). (c) To check whether LINC00263 is involved in miRISC, Ago2 RNP-IP was performed using specific antibody.

The level of LINC00263 in control IgG and Ago2 IP materials was determined by RT-qPCR analysis and normalized to the level of GAPDH mRNA. (d-f) To screen for LINC00263-associated miRNAs, antisense oligonucleotide pull-down (ASO PD) was performed. Schematic of the experimental design is shown (d). Detailed information of the ASO sequences for LacZ (control) and LINC00263 was provided into Supplementary fig. 4a. Efficiency of ASO PD was examined by comparing the level of LINC00263 in ASO PD materials (e). Small RNA sequencing was performed with RNAs isolated from ASO PD materials. miRNAs with higher expression in LINC00263 ASO PD are listed (f and Supplementary fig. 4b). (g-j) HeLa cells were transfected with pre-miR-147a (for overexpression, g and i) or anti-miR-147a (for inhibition, h and j). Direct association of LINC00263 with miR-147a-involved miRISC was analyzed by Ago2 RNP-IP (g-h) and the level of LINC00263 was determined by RT-qPCR analysis (i-j). (k) Following knockdown of hnRNPK and LINC00263, the level of miR-147a was determined by RT-qPCR analysis. (l) Bioinformatic analyses revealed that two MREs of miR-147a exist in LINC00263 sequence (Supplementary fig. 7a and 7b). To examine the sequence-specific interaction, luciferase reporter vectors containing wild-type or mutant sequences of miR-147a MREs were constructed. Following overexpression of miR-147a, the luciferase activity was assessed as described in Materials and methods. (m-r) To investigate the effect of miR-147a on malignant capabilities, pre-miR-147a (m, o, and q) or anti-miR-147a (n, p, and r) were introduced into HeLa cells. Malignant phenotypes including invasiveness (m-n), proliferation rate (o-p), and clonogenicity (q-r) were examined as described in Materials and methods. Bars on microscopic images represent 100 μm. Statistical analyses were performed using the Student’s t-test using three independent experiments (* $p < 0.05$). All data represent mean ± standard variation (SD).

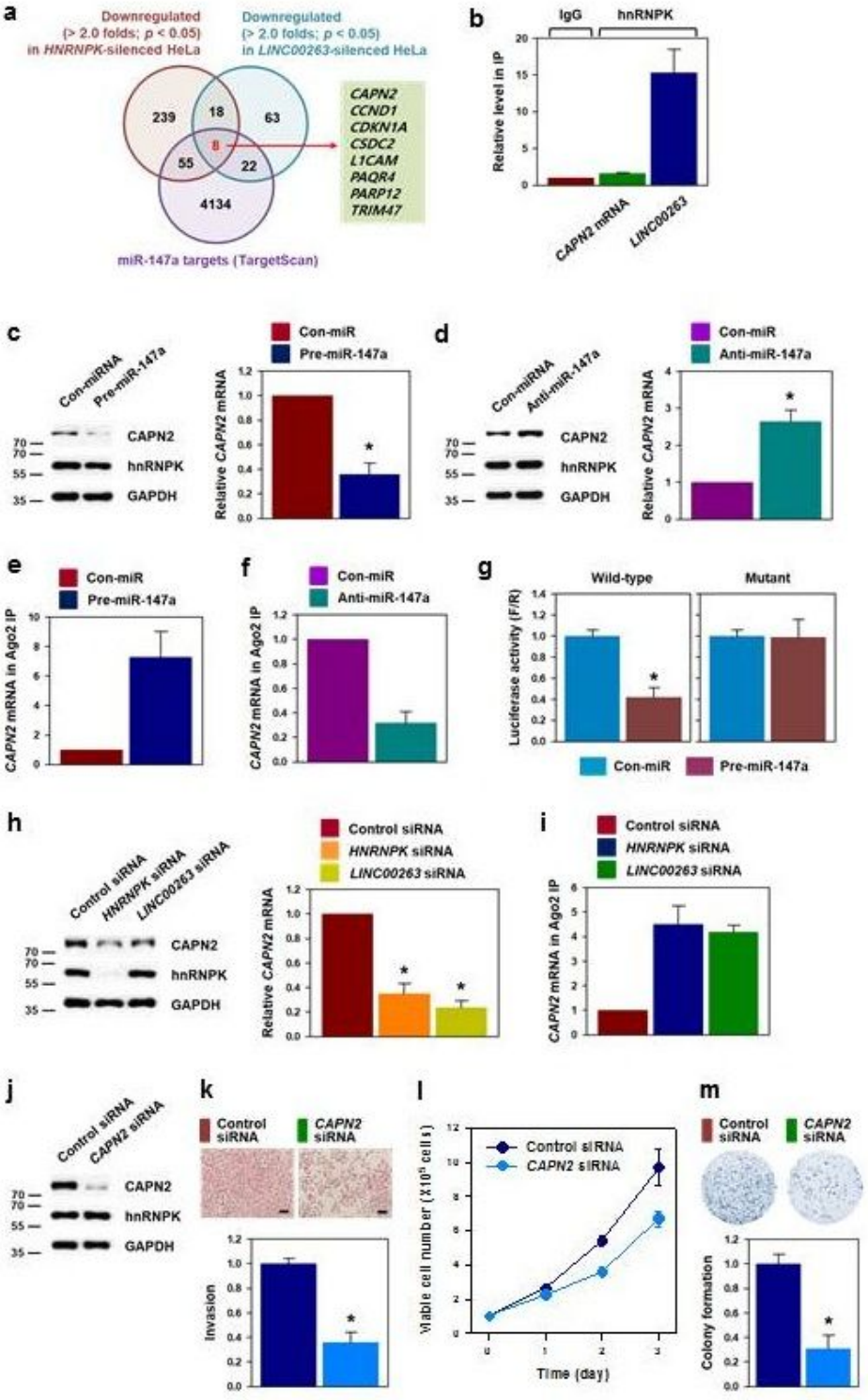

Figure 5

CAPN2 is responsible for the oncogenic function of hnRNPK/LINC00263/miR-147a. (a) By comparing RNA sequencing data and miR-147a predicted target genes (TargetScan v7), eight genes were selected as putative targets of hnRNPK/LINC00263/miR-147a. (b) To check whether interaction of hnRNPK with CAPN2 mRNA is required for the regulation of its expression, RNP-IP experiment was performed. The levels of CAPN2 mRNA and LINC00263 in each IP material were determined by RT-qPCR analysis. (c-g)

Following transfection of HeLa cells with pre-miR-147a (for overexpression, c, e, and g) or anti-miR-147a (for inhibition, d and f), the levels of CAPN2 protein and mRNA were determined by Western blot and RT-qPCR analyses, respectively. To examine whether miR-147a directly binds to the 3'UTR of CAPN2 mRNA, Ago2 RNP-IP (e-f) and luciferase reporter assay (g) were performed. Detailed information of luciferase reporter vector is presented in Supplementary fig. 7c. (h) Protein and mRNA expression of CAPN2 in hnRNPK- and LINC00263-silenced cells were determined by Western blot and RT-qPCR analyses, respectively. (i) To examine whether knockdown of hnRNPK or LINC00263 influences the interaction between miR-147a and CAPN2 mRNA, Ago2 RNP-IP assay was performed as described in Materials and methods. (j-m) The effect of CAPN2 silencing on malignant phenotypes including invasiveness (k), proliferation (l), and clonogenicity (m) were investigated. The efficiency of CAPN2 silencing was determined by Western blot analysis (j). Bars on microscopic images represent 100 μm. Statistical analyses were performed using the Student's t-test using three independent experiments (* $p < 0.05$). All data represent mean ± standard variation (SD).

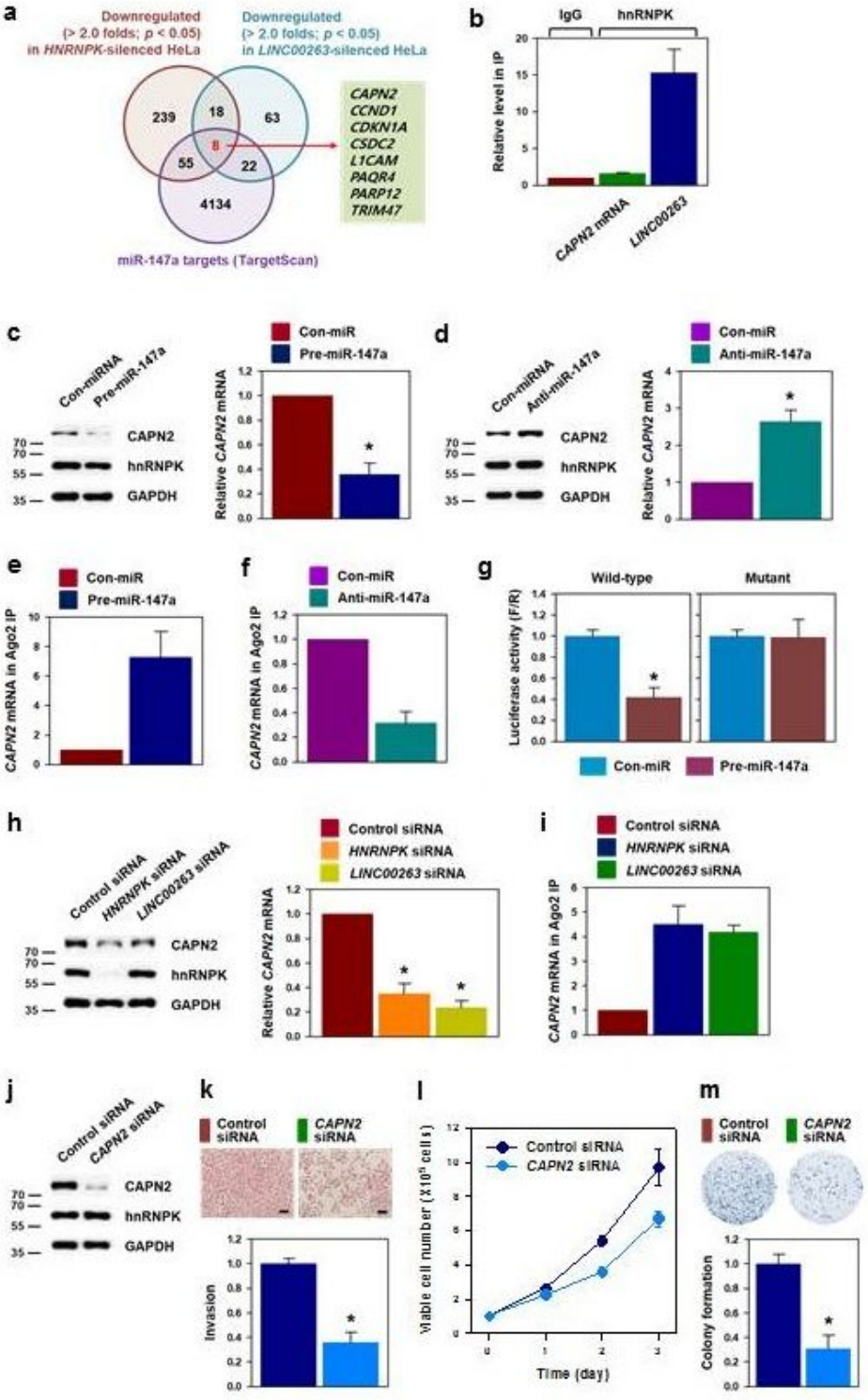

Figure 5

CAPN2 is responsible for the oncogenic function of hnRNPK/LINC00263/miR-147a. (a) By comparing RNA sequencing data and miR-147a predicted target genes (TargetScan v7), eight genes were selected as putative targets of hnRNPK/LINC00263/miR-147a. (b) To check whether interaction of hnRNPK with CAPN2 mRNA is required for the regulation of its expression, RNP-IP experiment was performed. The levels of CAPN2 mRNA and LINC00263 in each IP material were determined by RT-qPCR analysis. (c-g)

Following transfection of HeLa cells with pre-miR-147a (for overexpression, c, e, and g) or anti-miR-147a (for inhibition, d and f), the levels of CAPN2 protein and mRNA were determined by Western blot and RT-qPCR analyses, respectively. To examine whether miR-147a directly binds to the 3'UTR of CAPN2 mRNA, Ago2 RNP-IP (e-f) and luciferase reporter assay (g) were performed. Detailed information of luciferase reporter vector is presented in Supplementary fig. 7c. (h) Protein and mRNA expression of CAPN2 in hnRNPK- and LINC00263-silenced cells were determined by Western blot and RT-qPCR analyses, respectively. (i) To examine whether knockdown of hnRNPK or LINC00263 influences the interaction between miR-147a and CAPN2 mRNA, Ago2 RNP-IP assay was performed as described in Materials and methods. (j-m) The effect of CAPN2 silencing on malignant phenotypes including invasiveness (k), proliferation (l), and clonogenicity (m) were investigated. The efficiency of CAPN2 silencing was determined by Western blot analysis (j). Bars on microscopic images represent 100 μm. Statistical analyses were performed using the Student's t-test using three independent experiments (* $p < 0.05$). All data represent mean ± standard variation (SD).

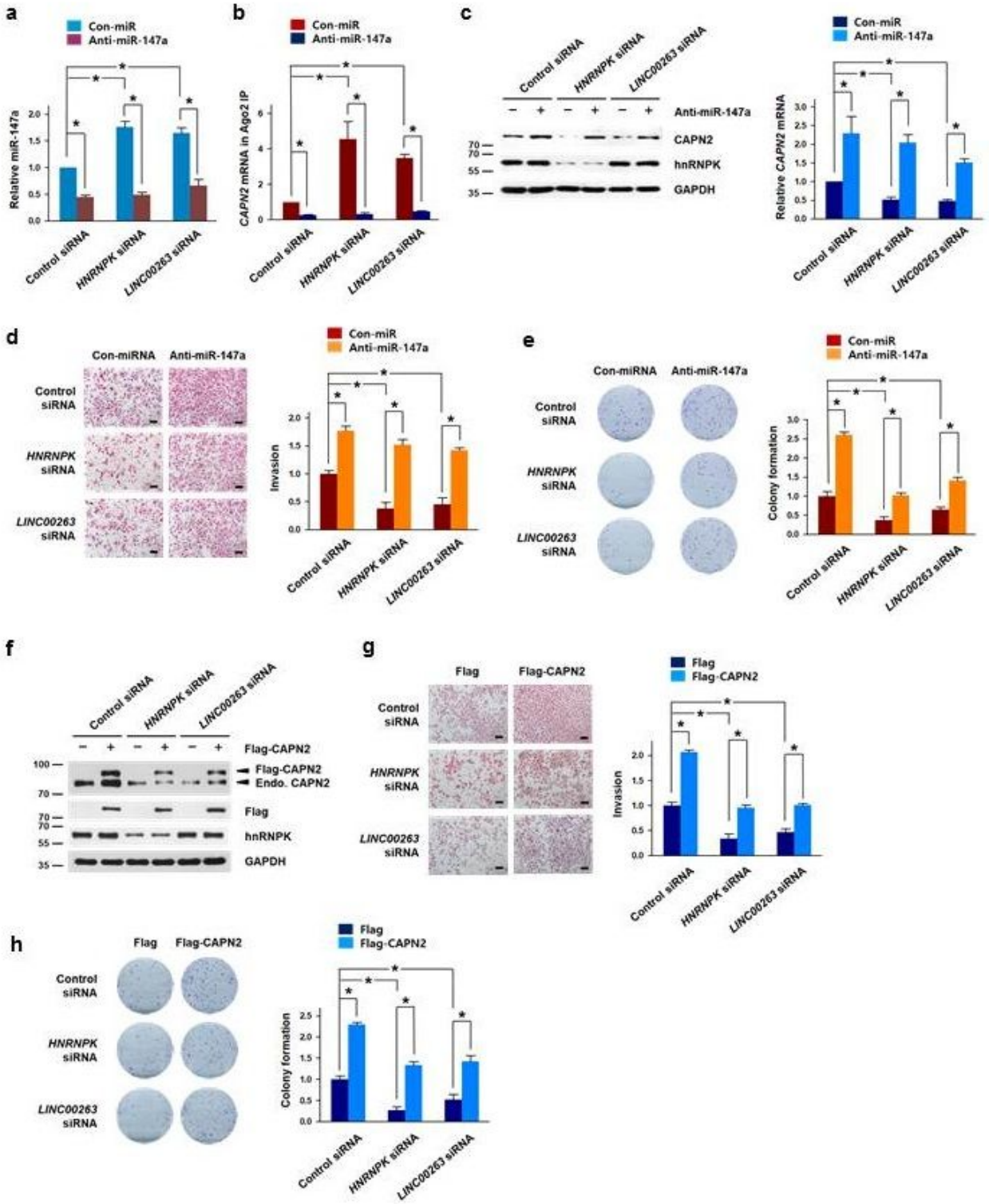

Figure 6

Repression of malignant phenotypes following knockdown of hnRNPK and LINC00263 is restored by inhibition of miR-147a or ectopic expression of CAPN2. (a-e) To examine whether inhibition of miR-147a restores the malignant capabilities, siRNAs for hnRNPK or LINC00263 were introduced into HeLa cells with control miRNA or anti-miR-147a. Following isolation of total RNA, the level of miR-147a was determined by RT-qPCR analysis (a). Ago2 RNP-IP experiment was performed using the cytoplasmic

lysates. The level of CAPN2 mRNA in Ago2 IP material was determined by RT-qPCR analysis (b). The expression levels of CAPN2 protein and mRNA were determined by Western blot and RT-qPCR analyses, respectively (c). Invasiveness (d) and colony forming ability (e) were examined as described in Materials and methods. (f-h) For the rescue experiments, CAPN2 was ectopically overexpressed in hnRNPK-or LINC00263-silenced HeLa cells. The protein level of CAPN2 was determined by Western blot analysis (f). Invasiveness (g) and colony forming ability (h) were examined as described in Materials and methods. Bars on microscopic images represent 100 μm. Statistical analyses were performed using the Student's t-test using three independent experiments (* $p < 0.05$). All data represent mean ± standard variation (SD).

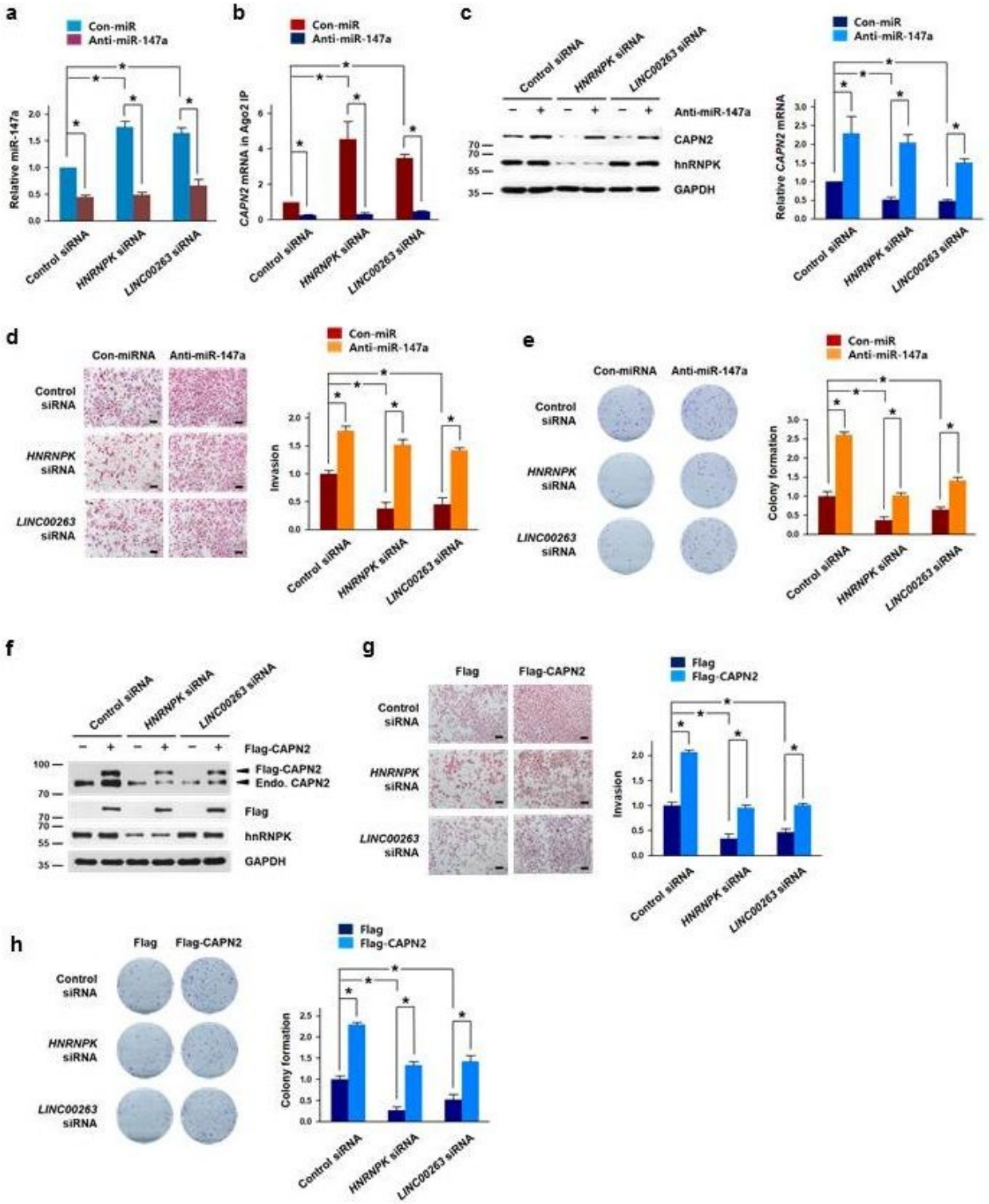

Figure 6

Repression of malignant phenotypes following knockdown of hnRNPK and LINC00263 is restored by inhibition of miR-147a or ectopic expression of CAPN2. (a-e) To examine whether inhibition of miR-147a restores the malignant capabilities, siRNAs for hnRNPK or LINC00263 were introduced into HeLa cells with control miRNA or anti-miR-147a. Following isolation of total RNA, the level of miR-147a was determined by RT-qPCR analysis (a). Ago2 RNP-IP experiment was performed using the cytoplasmic

lysates. The level of CAPN2 mRNA in Ago2 IP material was determined by RT-qPCR analysis (b). The expression levels of CAPN2 protein and mRNA were determined by Western blot and RT-qPCR analyses, respectively (c). Invasiveness (d) and colony forming ability (e) were examined as described in Materials and methods. (f-h) For the rescue experiments, CAPN2 was ectopically overexpressed in hnRNPK-or LINC00263-silenced HeLa cells. The protein level of CAPN2 was determined by Western blot analysis (f). Invasiveness (g) and colony forming ability (h) were examined as described in Materials and methods. Bars on microscopic images represent 100 μm. Statistical analyses were performed using the Student's t-test using three independent experiments (* $p < 0.05$). All data represent mean ± standard variation (SD).

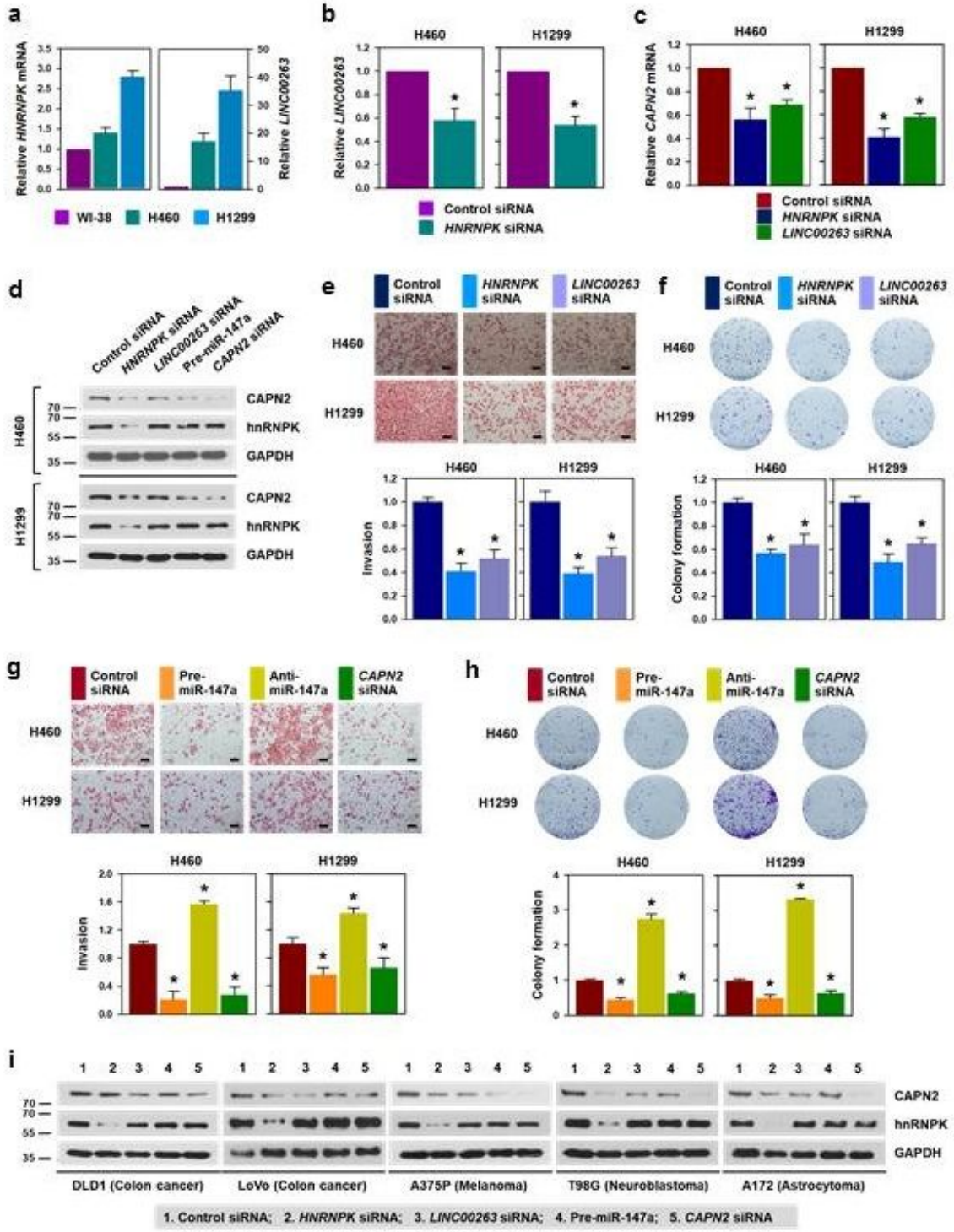

Figure 7

hnRNPK/LINC00263/miR-147a/CAPN2 is a promising target for the development of cancer therapeutics. To expand our findings to various types of cancer, we checked whether the regulatory mechanism of hnRNPK/LINC00263/miR-147a/CAPN2 is applicable to various types of cancers. (a) The relationship between the expression of HNRNPK mRNA and LINC00263 was examined in lung cancer cells by comparing them to the levels in WI-38 cells. The levels of HNRNPK mRNA and LINC00263 in WI-38, H460,

and H1299 were determined by RT-qPCR analysis. (b) To determine whether hnRNPK regulates LINC00263, the level of LINC00263 was analyzed by RT-qPCR analysis in hnRNPK-silenced lung cancer cells. (c) Regulation of CAPN2 by hnRNPK and LINC00263 was verified by assessing the level of CAPN2 mRNA in hnRNPK- or LINC00263-silenced lung cancer cells. (d-h) To examine whether hnRNPK/LINC00263/miR-147a/CAPN2 axis regulates the invasive and clonogenic abilities, H460 and H1299 cells were transfected with siRNA targeting HNRNPK mRNA or LINC00263, or pre-miR-147a. The level of CAPN2 protein was determined by Western blot analysis (d). Invasiveness (e and g) and colony forming ability (f and h) were examined as described in Materials and methods. (i) The effect of hnRNPK/LINC00263/miR-147a on CAPN2 expression was evaluated in various cancer cells including DLD1, LoVo, A375P, T98G, and A172. The expression level of CAPN2 and hnRNPK were determined by Western blot analysis. Bars on microscopic images represent 100 μm. Statistical analyses were performed using the Student's t-test using three independent experiments (* $p < 0.05$). All data represent mean ± standard variation (SD).

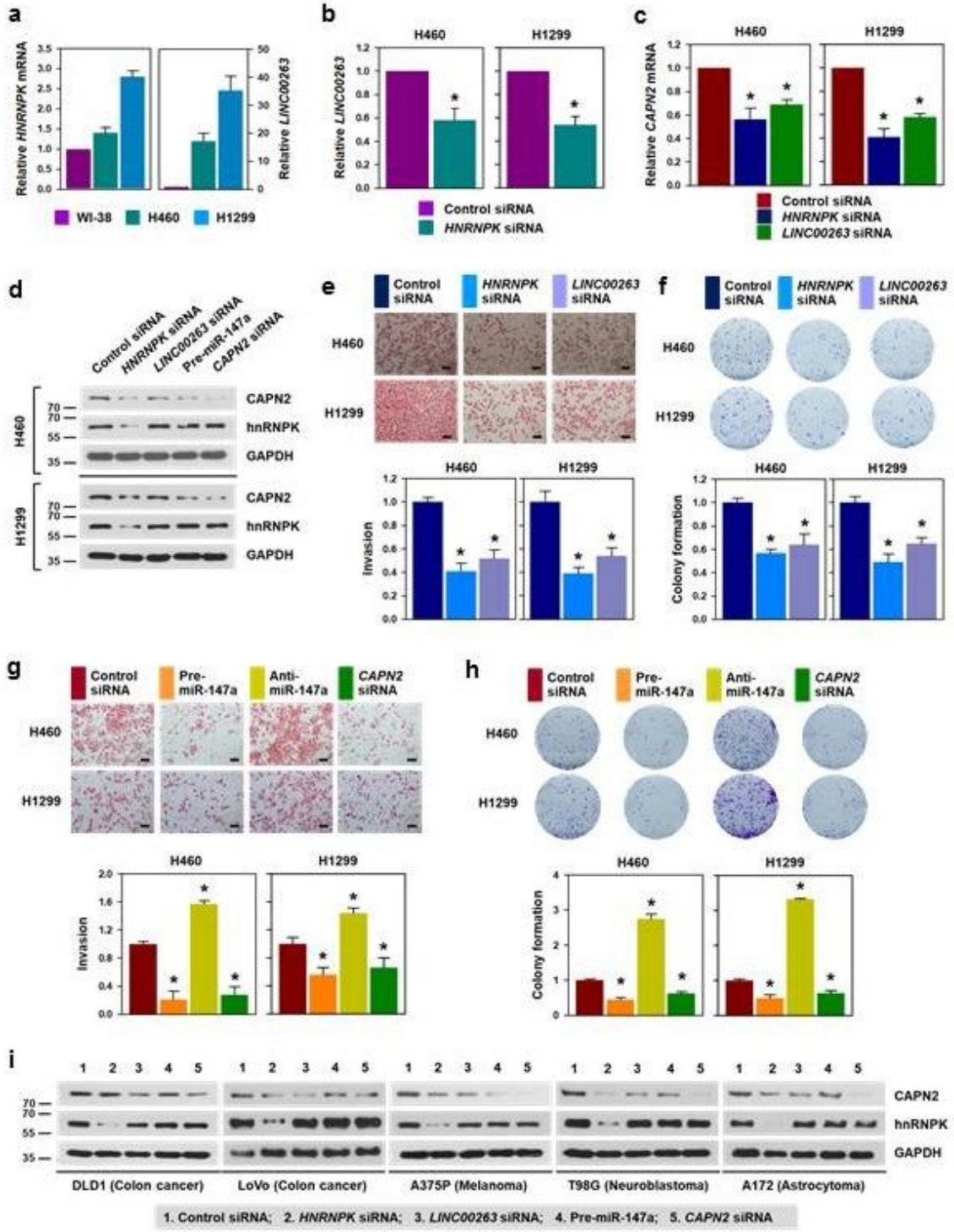

Figure 7

hnRNPK/LINC00263/miR-147a/CAPN2 is a promising target for the development of cancer therapeutics. To expand our findings to various types of cancer, we checked whether the regulatory mechanism of hnRNPK/LINC00263/miR-147a/CAPN2 is applicable to various types of cancers. (a) The relationship between the expression of HNRNPK mRNA and LINC00263 was examined in lung cancer cells by comparing them to the levels in WI-38 cells. The levels of HNRNPK mRNA and LINC00263 in WI-38, H460,

and H1299 were determined by RT-qPCR analysis. (b) To determine whether hnRNPK regulates LINC00263, the level of LINC00263 was analyzed by RT-qPCR analysis in hnRNPK-silenced lung cancer cells. (c) Regulation of CAPN2 by hnRNPK and LINC00263 was verified by assessing the level of CAPN2 mRNA in hnRNPK- or LINC00263-silenced lung cancer cells. (d-h) To examine whether hnRNPK/LINC00263/miR-147a/CAPN2 axis regulates the invasive and clonogenic abilities, H460 and H1299 cells were transfected with siRNA targeting HNRNPK mRNA or LINC00263, or pre-miR-147a. The level of CAPN2 protein was determined by Western blot analysis (d). Invasiveness (e and g) and colony forming ability (f and h) were examined as described in Materials and methods. (i) The effect of hnRNPK/LINC00263/miR-147a on CAPN2 expression was evaluated in various cancer cells including DLD1, LoVo, A375P, T98G, and A172. The expression level of CAPN2 and hnRNPK were determined by Western blot analysis. Bars on microscopic images represent 100 μm. Statistical analyses were performed using the Student's t-test using three independent experiments (* $p < 0.05$). All data represent mean ± standard variation (SD).

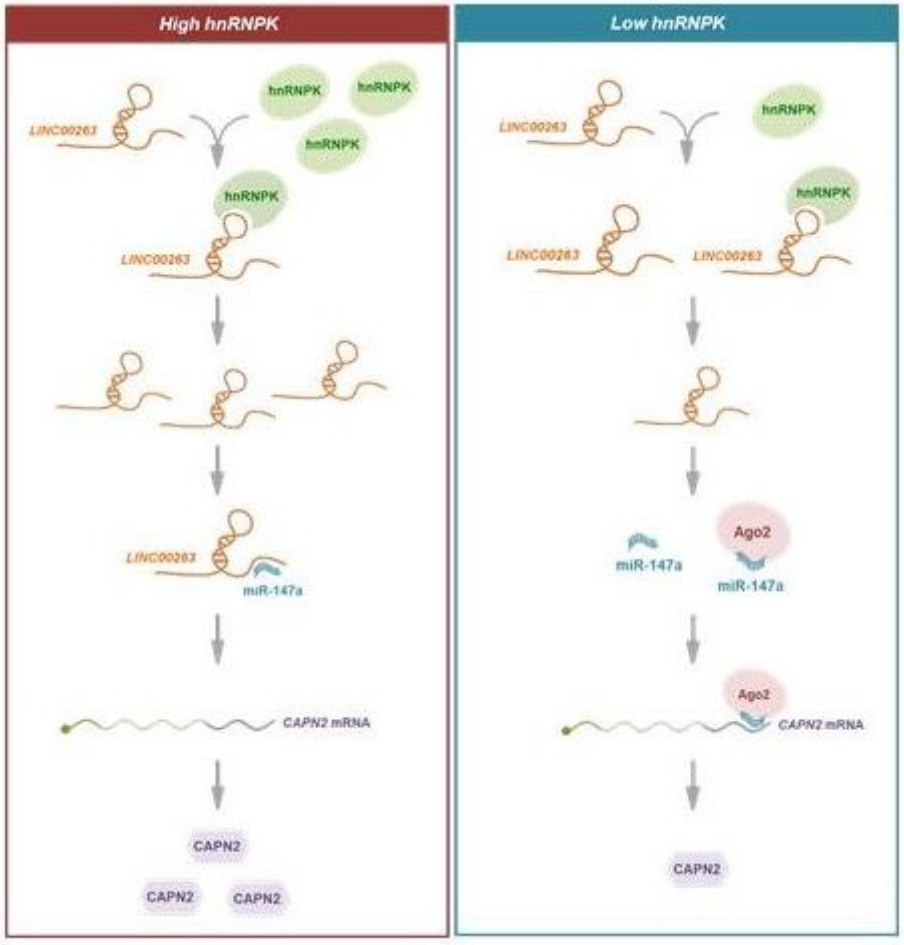

Figure 8

Schematic of the proposed mechanism of action of the oncogenic hnRNPK/LINC00263/miR-147a/CAPN2 axis. Detailed description is provided in the main text.

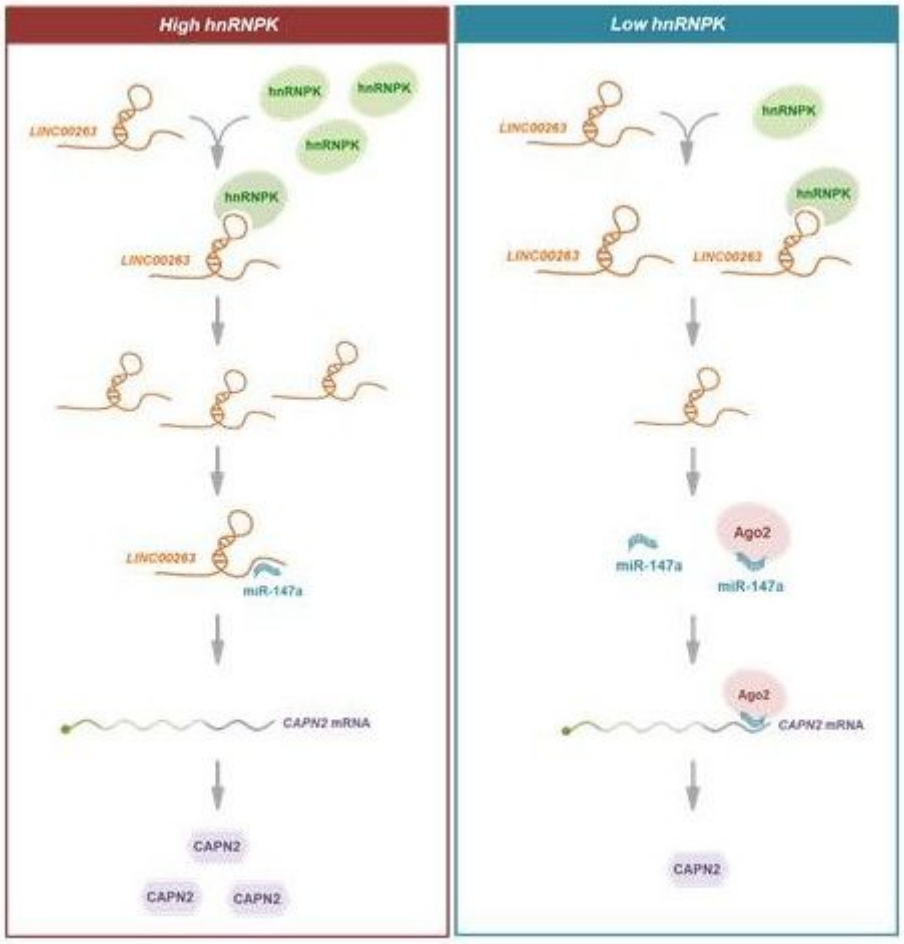

Figure 8

Schematic of the proposed mechanism of action of the oncogenic hnRNPK/LINC00263/miR-147a/CAPN2 axis. Detailed description is provided in the main text.

Supplementary Files

This is a list of supplementary files associated with this preprint. Click to download.

- AdditionalfileLINC00263hnRNPKJExpClinCancerRes.pptx
- AdditionalfileLINC00263hnRNPKJExpClinCancerRes.pptx